[American Journal of Science, Vol. 318, May, 2018, P. 491–526, DOI 10.2475/05.2018.03]

# THE IRON PALEOREDOX PROXIES: A GUIDE TO THE PITFALLS, PROBLEMS AND PROPER PRACTICE

ROB RAISWELL*,†, DALTON S. HARDISTY**, TIMOTHY W. LYONS***, DONALD E. CANFIELD§, JEREMY D. OWENS§§, NOAH J. PLANAVSKY§§§, SIMON W. POULTON*, and CHRISTOPHER T. REINHARD‡

**ABSTRACT. Oceanic anoxia—including euxinic settings defined by the presence of water column hydrogen sulfide ($H_2S$)—is minor in the ocean today. Such conditions, however, were common or even dominant in the past, particularly during the Precambrian and Phanerozoic oceanic anoxic events. The latter are associated with massive petroleum and mineral reserves and many of the major extinction events in the paleontological record. Our ability to recognize ancient oxygen deficiencies relies strongly on paleontological data viewed in combination with geochemical tracers, and geochemistry is typically our only window onto ancient marine redox during the Precambrian when diagnostic skeletal and behaviorial traces of oxygen-dependent animals are mostly missing. So far no approach has gained wider acceptance than the iron proxies, which rely generally on quantification of the extent to which reactive iron (as oxides principally) is converted to pyrite. The promise of these approaches lies in part with the relative ease of measurement, but it is this ease and the corresponding widespread use that has also led to misuses.**

**Much of the recent confidence in the iron paleoredox proxies lies with sophisticated deconstruction of the reactive Fe pool via mineral-calibrated wet chemical speciation. These validations and calibrations, mostly in the modern ocean, expose the challenges, while at the same time opening other doors of opportunity as the catalog of controlling factors extends beyond water column redox to include sedimentation rate, sedimentary Fe remobilization, signals of oscillatory redox, and hydrothermal versus other primary Fe inputs to the ocean, among other factors. Also key is a deep understanding of the limitations imposed—or at least the due diligence required—as linked to mineral transformations during burial and metamorphism. This review seeks to highlight many of the key issues, including appropriate sample choices, as a roadmap for those keen to apply Fe proxies in their studies of ancient oceans and their relationships to co-evolving life. Among the critical messages to take away is the value of robust Fe-based measures of local redox that, when combined with elemental mass balances and isotopic proxies dependent on those local conditions, can shed light on the global redox state of the oceans through time and related implications for the history of life on Earth.**

Key words: iron paleoredox proxy, iron geochemistry

## INTRODUCTION

Iron geochemistry has arguably become the most widely used approach to assess local oxygen conditions in ancient marine environments. These Fe-based methods have heightened utility because of studies over the past two decades that have explored their mechanistic underpinnings, particularly in modern analog settings, and through

* School of Earth and Environment, Leeds University, Leeds LS2 9JT, United Kingdom
** Department of Earth and Environmental Sciences, Michigan State University, East Lansing, Michigan 48824, USA
*** Department of Earth Sciences, University of California Riverside, California 92521, USA
§ Nordic Center for Earth Evolution, Department of Biology, Campusvej 55, 5230 Odense M, Denmark
§§ Department of Earth, Ocean and Atmospheric Science, Florida State University, Tallahassee, Florida 32306-4520, USA
§§§ Department of Geology and Geophysics, Yale University, New Haven, Connecticut 06520, USA
‡ School of Earth & Atmospheric Sciences, Georgia Institute of Technology, 311, First Drive, Atlanta, Georgia 30332-0340, USA
† Corresponding author: R.W.Raiswell@leeds.ac.uk

increased interest in time periods, particularly in the Precambrian, when paleoredox is otherwise difficult to assess in the absence of unambiguously diagnostic fossils. Added value has also come from coupling of Fe-based paleoredox proxies with other methods, such as trace metal geochemistry and isotope work, that together yield more convincing, and often more nuanced, views of ancient aquatic settings on a range of spatial scales. These iron methods are grounded in careful development of a sequential wet chemical extraction scheme calibrated against pure mineral phases and through extensive analysis of modern marine sediments, wherein direct measures of the oxygen and hydrogen sulfide availability in the water column are possible. In very simple terms, the methods are predicated on the observation that iron-bearing mineral phases (oxides and carbonates in particular) that are reactive toward hydrogen sulfide on short, diagenetic time scales are enriched relative to the total iron pool in sediments deposited beneath anoxic waters that are either ferruginous or sulfidic (see Appendix for definitions). Furthermore the extent to which this iron is converted to pyrite (see Appendix) ties closely to the presence or absence of sulfide. However, since the iron proxies are empirically calibrated they can be misapplied and care must be taken to ensure that the samples being analyzed are equivalent in fundamental ways (for example, lithology) to those against which the proxies were calibrated.

A major strength of the iron proxies is the ease with which data can be generated on relatively small samples. Prior to the development of these proxies, different depositional redox environments were recognized by paleoecological or micropaleontological techniques, organic geochemical indicators, carbon-sulfur relationships, or combinations of isotopic data and mineralogy. All of these methods had disadvantages arising from fossil preservation/availability issues, sample size, time-consuming separations, expensive instrumentation, or ambiguities due to compositional effects (Raiswell and others, 1988). With the emergence of the first of the iron proxies, the Degree of Pyritization (see Appendix), many of these difficulties were overcome; sample sizes were small, the analytical methodology was simple and required only basic instrumentation, and the method was supported by earlier studies of Fe mineral diagenesis in modern marine sediments. Despite this important step forward, complications soon emerged, leading to the development of refined proxies (Poulton and Canfield, 2005), but additional steps remain to be taken. As will be seen below, there are many issues that require further consideration, such as the impact of high sedimentation rates, fluctuating redox conditions, iron enrichment mechanisms, diagenetic/metamorphic remobilization, and mineralogical/lithological variations.

In recent years, we have observed examples where these wide ranging concerns are not considered adequately. Crucially, we have learned that proxies should be considered in a holistic context to optimize interpretations, a message that will be repeated in the examples that follow. Our goal in this review is to walk through the various iron proxies, provide historical context on their development (for more detail on this see Raiswell and Canfield, 2012), and to illustrate, through a set of case studies, ways in which the proxies can forward our understanding—or lead to ambiguous conclusions. It is not our intent to provide a comprehensive critique of all recent applications of the iron proxies. Rather, our aim is to build a foundation that captures the state of the art while also offering suggestions for best practices as the field moves forward. A glossary in the Appendix provides working definitions of relevant terms used throughout the text.

## DEGREE OF PYRITIZATION

The Degree of Pyritization (DOP) was originally developed to explore the effects of iron limitation on pyrite formation in modern marine sediments (Berner, 1970) and was only subsequently used to recognize the degree of bottom water oxygenation in organic carbon-bearing marine sediments and ancient rocks (Raiswell and others,

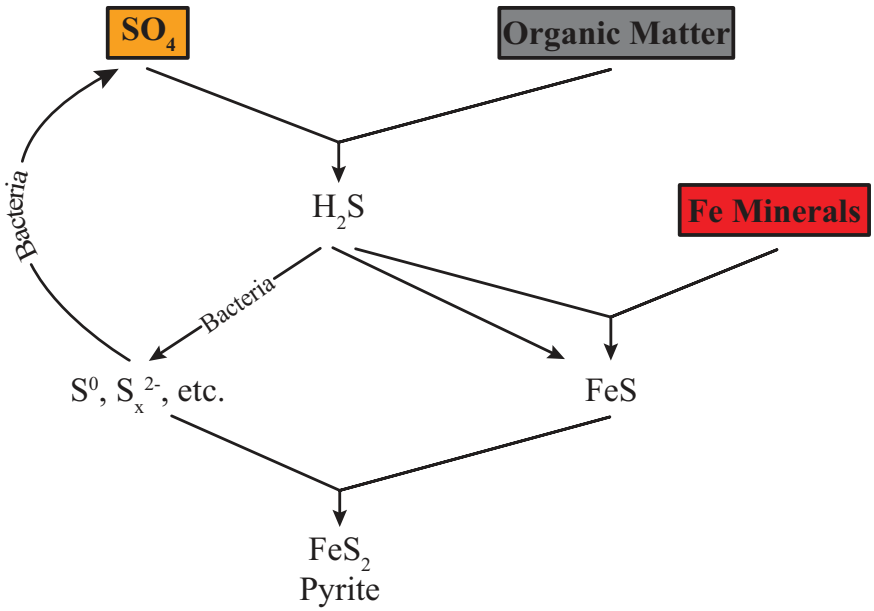


Fig. 1. Schematic model of pyrite formation (after Berner, 1984 and Hurtgen and others, 1999). $H_2S$ produced by sulfate reduction reacts with Fe minerals to form FeS, which then reacts with partially oxidized sulfide species. FeS can also react directly with $H_2S$ to produce pyrite.

1988). The foundation here is that pyrite formation requires three major components—iron, organic carbon, and sulfate—and each component can limit pyrite formation as a function of the first-order environmental conditions (fig. 1). Specifically, fresh waters and some early Precambrian marine systems may be limited in their supplies of sulfate. Organic carbon content controls pyrite formation in anoxic, non-sulfidic porewaters beneath oxic bottom waters (sometimes termed normal marine, following Raiswell and others, 1988), while iron limitation is indicated when sulfide builds up in those porewaters. Finally, iron is always limiting within and beneath anoxic/sulfidic (euxinic; see Appendix) bottom waters (Berner, 1984; Raiswell and Berner, 1985). In anoxic bottom waters and porewaters, anaerobic microbes initiate the process of pyrite formation through sulfate reduction—and the more organic C present, the more hydrogen sulfide produced and pyrite formed (until iron becomes limiting). Within this framework, we can imagine that Degrees of Pyritization, and thus extents of Fe limitation, could straightforwardly fingerprint ancient euxinia, and so methods were developed that allow us to quantify different Fe mineral pools.

DOP was defined by Berner (1970) as:

$$\mathrm{DOP} = \frac{\text{Pyrite Fe}}{\text{Pyrite Fe} + \text{HCl–soluble Fe}} \qquad (1)$$

where HCl-soluble Fe is extracted using concentrated HCl (table 1). This method completely dissolves fine-grained iron (oxyhydr)oxides, magnetite, and iron carbonates and partially extracts iron from some silicates (micas and clays in particular), such as nontronite, chlorite, and biotite (Raiswell and others, 1994). This HCl-soluble iron was assumed to provide a rough measure of the sediment iron that was reactive towards sulfide. It was hypothesized (Raiswell and others, 1988) that DOP might increase through increased consumption of HCl-soluble Fe in depositional

TABLE 1

*Commonly used extractions and the main minerals extracted (for methodology see Poulton and Canfield, 2005)*

| Extraction | Main Minerals Extracted |
|---|---|
| Na acetate, pH 4.5, 24 hr | Carbonate Fe, including siderite and ankerite |
| Na dithionite, pH 4.8, 2 hr | Ferrihydrite, lepidocrocite, goethite, hematite |
| $NH_4$ oxalate, pH 3.2, 6 hr | Magnetite |
| Boiling 12 N HCl, 2 mins | All Fe (oxyhydr)oxides, carbonate Fe and some silicate iron |

environments where there is increased opportunity for exposure to dissolved sulfide, such as sites marked by euxinia. DOP was subsequently measured in a range of Jurassic, Cretaceous, and Devonian sediments from depositional environments that were grouped into three categories representing a range of decreasing bottom water oxygenation:

(1) Aerobic (normal marine): homogeneous bioturbated sediments with trace fossils and an abundant and diverse benthic fauna dominated by epifaunal bivalves. These sediments were deposited from bottom waters that were fully oxygenated.
(2) Restricted (normal marine): poorly laminated sediments with sparse bioturbation and bivalves mainly comprising infaunal deposit feeders. Bottom waters were poorly oxygenated or fluctuated between oxic and anoxic.
(3) Inhospitable bottom water: finely laminated sediments with little or no bioturbation and a benthic fauna, if present, comprised of epifaunal suspension feeders. Bottom waters were anoxic (contained no dissolved oxygen).

The aerobic normal marine sediments (hereafter termed oxic) had values of DOP $<0.45$ and were clearly separated from restricted (hereafter dysoxic; see Appendix) samples with DOP values ranging from 0.45 to 0.80. Samples with inhospitable bottom waters contained only a very limited fauna and must have been mostly anoxic but were not necessarily sulfidic (euxinic). There was some overlap in samples from dysoxic and inhospitable bottom waters (hereafter anoxic, with DOP values of 0.55–0.93), but a boundary at 0.75 separated more than 90 percent of the samples from these two sets. The overlapping DOP values were attributed to temporal fluctuations between low oxygen and anoxic conditions, suggesting that unambiguous proxy signals can only result from stable depositional environments. Finally, the relatively high DOP values in most anoxic samples were attributed to the presence of sulfide in the bottom waters, which provided an opportunity for detrital iron minerals to react with dissolved sulfide both in the water column and during burial after deposition. In other words, high euxinic DOP values, approaching unity, were thought to result from nearly complete pyritization of all the HCl-extractable iron—thanks to its long exposure to sulfide in the water column, on the seafloor, and during burial.

The idea that protracted sulfide exposure alone explains the high DOP values of euxinic sediments turned out to be incorrect. The explanation lies instead with the unique iron properties of such settings. Most pyrite forms from iron (oxyhydr)oxide minerals that are reactive towards sulfide on timescales of less than a year, whereas many other iron minerals react, if at all, on timescales of thousands of years (Canfield, 1989; Canfield and others, 1992; Raiswell and Canfield, 1996). For example, the iron extracted by HCl from nontronite, chlorite, and biotite (see Berner, 1970) is scarcely

able to react with $H_2S$ to form pyrite, and thus the measurements of HCl-soluble Fe by Raiswell and others (1988) include minerals that cannot be significantly pyritized. Consistent with this, Canfield and others (1992) found that all the iron (oxyhydr)oxides were sulfidized in the sediments from the Friends of Anoxic Mud (FOAM) site in Long Island Sound, but only intermediate DOP values (~0.40) were reached despite exposure to porewater sulfide concentrations of up to 6 mM for *thousands of years* (see Case Study 1 and Hardisty and others, 2018). These data show that high DOP values in euxinic sediments could not arise as a result of exposure of poorly reactive HCl-soluble Fe minerals to high concentrations of sulfide for long periods of time. Instead, these high DOP values must result from elevated concentrations of the easily pyritized iron (oxyhydr)oxide minerals as compared to oxic sediments.

The potential for iron-bearing silicates to react with sulfide was further examined in separate Black Sea studies by Canfield and others (1996) for the deep basinal, euxinic sediments and by Lyons and Berner (1992) for shelf margin sediments and turbidites deposited rapidly under euxinic conditions. Canfield and others (1996) used a dithionite extraction (table 1) to search for iron (oxyhydr)oxide minerals, with negligible effects on the silicates that are partially dissolved in the overly aggressive boiling HCl (see Raiswell and others, 1994). This work, combined with pyrite extractions, showed that the Black Sea sediments contained very little unreacted (oxyhydr)oxide Fe but had 2 to 3 times more readily pyritized iron compared to typical continental margin sediments. The conclusion was that 'extra' highly reactive iron (see Appendix) was needed to produce high DOP values. Various mechanisms were suggested to explain how additional reactive iron could be derived from the water column.

The Lyons and Berner (1992) study found that shelf margin sediments and turbidites deposited rapidly under euxinic conditions, in contrast only reached intermediate DOP values (see Case Study 2). This relationship was attributed to their rapid deposition and the associated presence of smaller amounts of readily reactive iron compared to more slowly accumulating euxinic sediments, even though these sites of rapid deposition experienced long exposure to high levels of sulfide during burial. Conversely, high DOP values in the deep, slowly accumulating Black Sea basin were attained rapidly in the water column and in the uppermost sediment layers. This observation further confirmed that reactive iron enrichments (and not sulfide exposure) were necessary for high DOP values measured using the HCl method, while also asserting the need to consider the sedimentological context and the possible sources and controls for inputs of additional iron. These issues are the focus of discussions below. In conclusion, high values of DOP (>0.75) almost universally reflect euxinic conditions, and low values (<0.45) generally typify oxic depositional conditions. However, it is important to realize that intermediate values can arise both from fluctuating depositional environments and persistent exposure to sulfide-limited porewaters, as well as from rates of sedimentation that are sufficiently high to dilute the additional reactive iron under euxinic conditions (Lyons, 1997; Werne and others, 2002; Cruse and Lyons, 2004; Lyons and Severmann, 2006; Lyons and others, 2009).

Modern sediments with relatively high concentrations of AVS (Acid Volatile Sulfides; see Appendix) are better characterized by defining a Degree of Sulfidation (DOS; see Appendix), rather than DOP. DOS is derived by the addition of AVS-associated Fe to the numerator and denominator of DOP;

$$\mathrm{DOS} = \frac{\text{Pyrite Fe} + \text{AVS Fe}}{\text{Pyrite Fe} + \text{AVS Fe} + \text{HCl–soluble Fe}} \qquad (2)$$

DOS is preferred over DOP for euxinic systems when AVS is present in appreciable amounts (Boesen and Postma, 1988; Middelburg, 1991; Hurtgen and others, 1999; Lyons and Severmann, 2006). However we emphasize that the calibration of DOP is

empirical and that the paleoenvironmental boundary values cannot be directly used for DOS. The same is also true where HCl-soluble Fe is replaced by other Fe extractions or by total Fe.

Regardless of the above, DOP remains a valid paleoenvironmental proxy subject to the constraints listed below which will, however, be amended in the following discussions. From these collective observations, basic ground rules emerged:

(1) Appreciable organic C (>0.5%) should be present. Sediments low in organic C undergo little or no sulfate reduction, and, for example, freshwater (sulfate-limited) and oxic marine sediments can be impossible to distinguish. (Importantly, high amounts of pyrite with very low organic C can, in theory, be a fingerprint of euxinia).

(2) Fresh outcrop or drill material should be used to minimize the loss of pyritic sulfur by oxidative weathering. Ahm and others (2017) found that weathering losses of pyrite could be found even in freshly exposed rock and weathering effects were only completely absent in samples taken beneath a drill core surface.

(3) Sediments should contain sufficient fine-grained, clastic, iron-containing material. Raiswell and others (1988) suggested that clastics are sufficiently abundant as long as there is less than 65% skeletal debris, although recent work suggests that carbonate rocks may offer greater promise than suggested by this earlier work (see later).

(4) No additions or losses of sulfur should have occurred as a result of sediment maturation or metamorphism. The formation of metamorphic pyrrhotite will be considered in Case Study 5.

(5) Sediments containing late diagenetic, iron-rich concretionary carbonates should be avoided, as iron migration may have added substantial amounts of HCl-soluble Fe.

(6) Raiswell and Berner (1986) also suggested that sediments older than the Devonian should be avoided because their associations with more-reactive organic C (in the absence of poorly-metabolizable, terrestrial plant-derived organic C) produce more pyritic sulfur per unit of organic C. However, as will be discussed, there has been an increasing appreciation that the reactive iron flux to the sediment is the predominant control on DOP, and numerous studies have applied these methods to very old, even Precambrian rocks.

Constraints 1 to 5 exclude many common rock types such as coals, evaporites, and sandstones—also cherts and limestones with a low clastic content. The compositional constraints defined by (1) to (5) are re-visited below. Consistent with the idea that the reactive iron flux dominates DOP, Raiswell and Al-Biatty (1989) found the DOP boundary at 0.75 also separates early Paleozoic samples deposited in oxic or dysoxic bottom waters from those deposited under euxinic conditions.

### THE INDICATOR OF ANOXICITY ($Fe_{HR}/Fe_T$)

The iron extracted by boiling HCl includes iron present in minerals that are too recalcitrant to be pyritized, in turn suggesting the need for a more accurate measure of the iron that was truly highly reactive towards sulfide. The high DOP values observed in modern euxinic sediments (such as the Black Sea; Lyons and Berner, 1992; Canfield and others, 1996; Wisjman and others, 2001) were found to result from a larger pool of iron delivered as (oxyhydr)oxides (larger than that found in oxic sediments) and/or through additional iron supplied in the dissolved ferrous form. Iron as (oxyhydr)oxides (table 1) can be measured by a dithionite extraction (Canfield, 1989), thus allowing highly reactive iron ($Fe_{HR}$) to be defined as the dithionite-extractable iron (oxyhydr)oxides fraction ($Fe_{ox}$, with high potential to form pyrite) plus iron already present as pyrite ($Fe_{py}$). In contrast, the HCl-soluble Fe includes all the Fe minerals

TABLE 2

*Modern sediment proxy values (data from Anderson and Raiswell, 2004; Raiswell and Canfield, 1998)*

| Sediment | $Fe_{HR}/Fe_T$ | $Fe_{py}/Fe_{HR}$ |
|---|---|---|
| Black Sea | 0.70±0.19 | 0.88±0.02 |
| Cariaco Basin | 0.51±0.03 | 0.89±0.02 |
| Dysoxic or Fluctuating | 0.28±0.10 | 0.63±0.27 |
| Continental Margin + Deep Sea | 0.26±0.08 | 0.10±0.17 |

soluble in dithionite plus other more recalcitrant Fe minerals that cannot be pyritized – at least on short diagenetic time scales. *Importantly, the boiling HCl method should only be used to approximate $Fe_{HR}$ if authigenic iron silicates are present (see Case Study 6), otherwise false signals of reactive iron enrichment can be produced* (Wen and others, 2014).

Measuring $Fe_{HR}$ as $Fe_{ox} + Fe_{py}$, Raiswell and Canfield (1998) showed that modern oxic continental margin and deep sea sediments exhibit a range of $Fe_{HR}$ contents. Table 2 shows these $Fe_{HR}/Fe_T$ values (which define an Indicator of Anoxicity; see Appendix and Raiswell and others, 2001) for oxic, modern continental margin and deep sea sediments along with data from settings with fluctuating/dysoxic conditions and from the euxinic Black Sea and Cariaco Basin. Mean $Fe_{HR}/Fe_T$ ratios from continental margin and deep sea sediments (0.26±0.08) are similar to those from fluctuating/dysoxic sediments (0.28±0.10), but both are clearly separated from the Black Sea (0.70±0.19) and the Cariaco Basin (0.51±0.03). A threshold value of 0.38 was found to separate the highest oxic data from the lowest anoxic/euxinic ratios. However, intense weathering environments (high rainfall and temperatures) can produce higher $Fe_{HR}/Fe_T$ values (ranging up to 0.52; Shi and others, 2011; Raiswell and others, 2016); similarly high values occur through intense physical or biological re-working in marginal marine environments (Aller and others, 1986). As such, there is no *a priori* reason to regard the 0.38 threshold as a definitive boundary throughout Earth history, and values falling near this boundary should be regarded as ambiguous (as addressed in discussions below). Strongly elevated $Fe_{HR}/Fe_T$ ratios by definition identify anoxic water columns that are either ferruginous or euxinic, and dysoxic regimes (low oxygen but neither euxinic or ferruginous) and those with fluctuating dysoxic conditions are therefore not discernable from oxic environments (Raiswell and Canfield, 1998) and require additional tools to delineate (see table 2).

In recent years, $Fe_{HR}/Fe_T$ has been refined in response to an improved understanding of highly reactive iron (Poulton and others, 2004) based on the recognition that rocks often contain highly reactive iron minerals other than pyrite and iron (oxyhydr)oxides—in particular, magnetite, siderite, and ankerite. An analytical scheme was developed (Poulton and Canfield, 2005) to measure Fe present in these minerals, leading to a new definition of highly reactive Fe based on Fe present as carbonates ($Fe_{carb}$, sodium acetate-soluble Fe), oxides ($Fe_{ox}$, dithionite-soluble crystalline Fe oxides), magnetite ($Fe_{mag}$, oxalate-soluble Fe) and pyrite ($Fe_{py}$):

$$Fe_{HR} = Fe_{carb} + Fe_{ox} + Fe_{mag} + Fe_{py} \quad (3)$$

In the case of modern sediments $Fe_{HR}$ would also include the Fe present as AVS ($Fe_{AVS}$). This newer definition demands that we consider whether the threshold value defined earlier—based on $Fe_{HR}$ data that excluded $Fe_{carb}$ and $Fe_{mag}$—should be modified. There is no simple answer to this question. In some cases, the addition of

$Fe_{mag}$ may have little impact on $Fe_{HR}/Fe_T$ for typical oxic sediments (see Case Study 1; Hardisty and others, 2018; Goldberg and others, 2012). In other cases, $Fe_{mag}$ has been found to represent a significant fraction of $Fe_{HR}$ (for example, in some glacially derived sediments; März and others, 2012). From hereon all $Fe_{HR}$ data in our discussions are derived using the Poulton and Canfield (2005) methodology (unless otherwise specified).

This methodological issue may also be relevant to the observations of Poulton and Raiswell (2002), who examined the iron speciation of ancient sediments ranging in age from Ordovician to Jurassic and characterized as oxic (normal marine; Raiswell and Berner, 1986) on the basis of paleoecology and DOP values. Defining $Fe_{HR}$ as $Fe_{ox}$ + $Fe_{py}$ (that is, not including $Fe_{carb}$ and $Fe_{mag}$) they found that the mean $Fe_{HR}/Fe_T$ values for these Cretaceous, Jurassic, Silurian, Ordovician, and Cambrian sediments ranged from 0.13±0.06 to 0.17±0.11 (average 0.14±0.08)—values that are significantly lower (at the <0.1% confidence level) than those from modern sediments (0.26±0.08). Poulton and Raiswell (2002) attributed these low $Fe_{HR}/Fe_T$ values to reductive transformation of residual iron oxides remaining after pyrite formation to poorly reactive silicate Fe during burial. This process has been identified in a number of ancient settings and has been attributed to the transfer of unsulfidized $Fe_{HR}$ to poorly reactive sheet silicate Fe during early-late diagenesis in low-sulfate (and hence low sulfide) marine sediments (for example, Poulton and others, 2010; Cumming and others, 2013).

However, Farrell and others (2013) argued that this difference may be due to the inefficiency with which dithionite extracts iron carbonate and magnetite which produces low values of $Fe_{HR}$. This difficulty, they argued, may be common in Paleozoic rocks because lower sulfate concentrations in the oceans might have resulted in less conversion of $Fe_{HR}$ to pyrite, leaving residual $Fe_{HR}$ to form iron carbonate and magnetite. Thus, the presence of iron carbonate and magnetite in Paleozoic rocks examined by the sequential methodology of Poulton and Canfield (2005) could potentially produce higher mean $Fe_{HR}/Fe_T$ values, similar to those found in modern sediments (0.26±0.08) rather than the lower values (0.14±0.08) found by summing oxide and pyrite Fe only (see also Farrell and others, 2013). As a consequence, the oxic threshold in Paleozoic rocks should be re-evaluated using the sequential methodology of Poulton and Canfield (2005). In the interim a pragmatic solution to the determination of $Fe_{HR}$ in Paleozoic samples that excludes $Fe_{carb}$ and $Fe_{mag}$ could be a threshold value of <0.22 based on the mean plus one standard deviation (0.14±0.08) for Ordovician-Jurassic sediments (Poulton and Canfield, 2011). However, this value is also not without risk because it assumes that iron carbonate and magnetite are insignificant. In response, Poulton and Canfield (2011) proposed that $Fe_{HR}/Fe_T$ ratios from 0.22 to 0.38 should be considered equivocal, as they could represent oxic conditions or anoxic conditions when high sedimentation rates have masked water column $Fe_{HR}$ enrichments or when $Fe_{HR}$ has been transferred to poorly reactive silicate Fe during diagenesis. Sperling and others (2016) point out that the lowest values of $Fe_{HR}/Fe_T$ in rapidly sedimented anoxic samples are ~0.2 (Raiswell and Canfield, 1998) and lower values are very likely to be oxic.

There are also important compositional constraints on use of the $Fe_{HR}/Fe_T$ ratio for the oxic/anoxic threshold in carbonate-rich sediments. Clarkson and others (2014) used the Poulton and Canfield (2005) methodology on sediments containing 65 to 80 percent carbonate, finding that the threshold $Fe_{HR}/Fe_T$<0.38 was valid as long as $Fe_T$ >0.5 percent. However, oxic, carbonate-rich sediments with $Fe_T$ <0.5 percent and organic C <0.5 percent routinely gave spuriously high $Fe_{HR}/Fe_T$ ratios that would falsely indicate deposition under anoxic conditions. Note also that analytical errors on iron species in carbonate-rich rocks (or any rocks with low values of $Fe_{HR}$

and/or $Fe_T$) may propagate through to produce values of $Fe_{HR}/Fe_T$ that apparently exceed threshold values (Ahm and others, 2017). Fluid alteration processes in carbonates also result in addition of iron (including the formation of Fe-rich dolomites), and we stress the need for caution in dealing with rocks altered by burial/metamorphic processes (see Case Study 5).

Values for $Fe_{HR}/Fe_T$ in dysoxic sediments are essentially similar to those in oxic sediments ($<0.38$), and, in general, integrated, multi-proxy geochemical approaches are required for recognizing fluctuations in bottom water oxygenation (Raiswell and Canfield, 1998). For example, Boyer and others (2011) examined Devonian black shales with paleontological data (ichnofabric index, species richness) that clearly show short-term fluctuations in bottom water oxygenation that fail to produce distinct shifts in $Fe_{HR}/Fe_T$. This situation arises because geochemical sampling of rocks inevitably homogenizes the geological record over a significant period of time, limiting our ability to recognize short-term redox variations. However, the paleontological data of Boyer and others (2011) were less useful when a combination of extremely low bottom water oxygenation and/or intermittent anoxia/euxinia precluded clear-cut biological signals. In these cases, finely laminated sediments failed to produce positive signals for anoxia or euxinia based on the threshold of $Fe_{HR}/Fe_T > 0.38$ (or by elevated values of other proxies, including DOP). In all cases threshold values should be applied with caution, with consideration as to depositional environment, sediment composition, and $Fe_{HR}$ extraction methodology.

### THE $Fe_T/Al$ RATIO

Alternative methods for detecting the iron enrichments that are diagnostic for anoxic/euxinic sediments were developed by Werne and others (2002), who used the $Fe_T/Ti$ ratio, and Lyons and others (2003), who used the $Fe_T/Al$ ratio. The $Fe_T/Al$ ratio is more widely used than $Fe_T/Ti$ (see Lyons and Severmann, 2006), and only the $Fe_T/Al$ is considered here—although the same principles apply to both. The $Fe_{HR}/Fe_T$ and $Fe_T/Al$ proxies assume that the enrichment of highly reactive iron is sufficient to produce a measurable and meaningful increase (relative to possible variation in the detrital baseline). Normalization (use of ratios) also allows for corrections for dilution by carbonate or silica-bearing biogenous sediment. The $Fe_{HR}/Fe_T$ and $Fe_T/Al$ indicators both track enrichments that arise from the addition of highly reactive iron, but only the former is sensitive to enrichments that arise from the conversion of an unreactive portion of $Fe_T$ to $Fe_{HR}$. The use of $Fe_T/Al$ ratios to detect iron enrichments requires a baseline against which enrichment can be assessed. A common threshold for this purpose are the $Fe_T/Al$ ratios in average shale, which range from 0.50 to 0.56 (for example Clarke, 1924; Ronov and Migdisov, 1971; Taylor and McLennan, 1985). Although these averages do not permit the use of statistical tests to assess the probability that an observed enrichment is significant, this problem can be overcome by using a mean and standard deviation for an appropriate $Fe_T/Al$ data set.

Raiswell and others (2008) found $Fe_T/Al$ to be $0.53 \pm 0.11$ (confidence limits hereon are for one standard deviation unless otherwise specified) in Paleozoic oxic marine shales. A more recent study (Clarkson and others, 2014) demonstrated that the $Fe_T/Al$ ratio averaged $0.55 \pm 0.11$ in modern marine sediments deposited under oxic conditions and that this value was independent of carbonate content (up to 80%). Cole and others (2017) estimated a $Fe_T/Al$ ratio for 4850 soils collected over a wide area of the continental USA. This data set averaged $0.47 \pm 0.15$ which Cole and others (2017) suggest should be used in conjunction with a confidence limit of two standard deviations ($0.47 \pm 0.30$)—in effect defining enrichment as $Fe_T/Al > 0.77$. Our preference is to use the sediment data base threshold with a confidence limit of one standard deviation (and thus to define enrichment as $Fe_T/Al > 0.66$) and to require supporting proxy or geological evidence for enrichment.

However, the best approach is to define an oxic threshold for any particular geological setting (Lyons and others, 2003; Lyons and Severmann, 2006; Poulton and others, 2010; Sperling and others, 2013; Clarkson and others, 2014). For example, Neoproterozoic samples from the Fifteen Mile Group (Sperling and others, 2013) had a mean $Fe_T/Al$ ratio of 0.34 with variations occurring down to $Fe_T/Al \sim 0.20$; similarly samples from the Windermere Supergroup (Sperling and others, 2016) had $Fe_T/Al$ of $0.32 \pm 0.17$ also with variations down to ~0.2 or less. Clearly it is optimal to consider local detrital $Fe_T/Al$ for a given locality.

The level of enrichment reflected in the $Fe_T/Al$ ratio depends on the geologic setting and the mechanism of enrichment, but values rising above 0.66 are conservatively diagnostic of enrichment (whether via chemocline addition, euxinia, or hydrothermal activity; see Case Studies 2 and 3). Large and variable enrichments have been found at hydrothermal sites close to mid-ocean ridges ($Fe_T/Al = 3.0 \pm 3.8$; Clarkson and others, 2014). Over half these samples had $Fe_T/Al > 2.0$ and it seems that $Fe_T/Al$ values above 2.0 most often arise from hydrothermal addition (see Case Study 4). A cautionary note arises because Fe enrichments can be swamped at high siliciclastic sedimentation rates (see Lyons and Severmann, 2006).

## THE $Fe_{py}/Fe_{HR}$ RATIO

The $Fe_{py}/Fe_{HR}$ indicator tracks the extent to which $Fe_{HR}$ is converted to pyrite. Poulton and others (2004) were the first to use $Fe_{py}/Fe_{HR,}$ stating that values $0.87 \pm 0.04$ were consistent with those found in modern euxinic sediments by Anderson and Raiswell (2004). Canfield and others (2008) concluded that values commonly exceeded 0.8 based on the euxinic data ($0.80 \pm 0.06$) in an unpublished database compiled for Raiswell and Canfield (1998). This ratio reaches values >0.70 to 0.80 in two fundamentally different settings: under euxinic conditions and in the sediments of oxic continental margins where porewaters accumulate sulfide at depth, resulting in near complete conversion of $Fe_{HR}$ to $Fe_{py}$ (see Case Study 1). These two scenarios can be distinguished by considering the $Fe_{py}/Fe_{HR}$ ratio in conjunction with $Fe_{HR}/Fe_T$ and $Fe_T/Al$; oxic continental margin sediments have $Fe_{HR}/Fe_T < 0.38$ and detrital $Fe_T/Al$ ratios, whereas euxinic sediments have $Fe_{HR}/Fe_T > 0.38$ and elevated $Fe_T/Al$. Poulton and others (2004) used $Fe_{py}/Fe_{HR}$ (at >0.80) to distinguish euxinicity from ferruginous conditions (indicated by $Fe_{py}/Fe_{HR} < 0.80$ in combination with $Fe_{HR}/Fe_T > 0.38$).

As mentioned earlier, this assessment of the $Fe_{py}/Fe_{HR}$ threshold is based on modern sediments for which $Fe_{mag}$ and $Fe_{carb}$ were not determined. Having results for $Fe_{carb}$ and $Fe_{mag}$ in these (or other) euxinic samples would be an important next step. In their absence, the data in table 3 show that the mean $Fe_{py}/Fe_{HR}$ for the Black Sea is $0.88 \pm 0.02$ (with only five measurements below 0.80) and $0.89 \pm 0.02$ for the Cariaco Basin. However, addition of as little as 0.10 percent of ($Fe_{mag} + Fe_{carb}$) to the $Fe_{HR}$ values for the Black Sea sediments would be sufficient to decrease the mean $Fe_{py}/Fe_{HR}$ to 0.81 (with 40% of the values below 0.80). A recent study of Phanerozoic euxinic sediments that included $Fe_{mag} + Fe_{carb}$ suggested a slightly lower threshold value of 0.70 for $Fe_{py}/Fe_{HR}$ (see Case Study 4 and Poulton and Canfield, 2011). In this light, we agree that the 0.70 threshold of Poulton and Canfield (2011) may be more appropriate, while sharing their greater confidence in values >0.80. *Most importantly, we emphasize that these thresholds should not be held as absolutes* and encourage caution during interpretations of data falling on or near the transitions. Many common circumstances, such as fluctuating redox conditions, can yield exceptions to these rules, demanding interpretation in light of other data, including a strong geologic context.

TABLE 3

*Best practice thresholds for the iron proxies*

| | | Best Practice Thresholds | | |
|---|---|---|---|---|
| **Environment** | **DOP*** | **$Fe_T/Al$**** | **$Fe_{HR}/Fe_T$**$^{+}$** | **$Fe_{py}/Fe_{HR}$**$^{++}$** |
| Oxic, Dysoxic | <0.45 | 0.55±0.11 | <0.22 or 0.38 | <1.0 |
| Anoxic, Ferruginous | <0.75 | >0.66 | 0.22(0.38) to >0.7 | 0.22(0.38)-0.7 |
| Euxinic | >0.75 | >0.66 | >0.7 | >0.7 |

* See DOP section; consider constraints 1–5.

** See $Fe_T/Al$ section; consider local thresholds and dilution effects. Hydrothermal inputs possible for $Fe_T/Al > 2$.

$^{+}$ See $Fe_{HR}/Fe_T$ section; consider compositional constraints ($Fe_T > 0.5\%$, organic C >0.5%). Modern sediment values in brackets.

$^{++}$ See $Fe_{py}/Fe_{HR}$ section; consider in conjunction with $Fe_T/Al$ and $Fe_{HR}/Fe_T$. Modern sediment values in brackets.

## PROXIES: THE GROUND RULES

The previous sections have drawn attention to important observations that apply to all applications of the iron proxies. These are listed below and then are examined in more detail in the Case Studies that follow:

- The iron proxies should be interpreted within a broad sedimentological and paleoecological context, taking into account rates of deposition and the extent of reworking by physical or biological processes.
- The threshold values defined for $Fe_{HR}/Fe_T$, $Fe_{py}/Fe_{HR}$, and $Fe_T/Al$ are not prescriptive, and areas of doubt exist. Specifically, ambiguous signals may occur in environments of marginal or fluctuating redox, settings affected by rapid detrital sedimentation, or due to post-depositional transformation of unsulfidized $Fe_{HR}$ to poorly reactive silicate Fe.
- Use of the proxies is particularly risky in cases where measured values of $Fe_T$ or organic C are small (<0.50%).
- Samples should be examined petrographically/mineralogically for evidence of $Fe_T$ (and $Fe_{HR}$) and S secondary mobilization (that is, loss or addition during burial or metamorphism).

With these caveats in mind, table 3 and figure 2 present the current best practice threshold values for the iron proxies.

## CASE STUDY 1: INSIGHTS FROM DETAILED SPECIATION STUDIES

Raiswell and Canfield (1998) originally defined $Fe_{HR}$ as the sum of pyrite Fe and the Fe extracted by dithionite. More recently, however, detailed speciation data from multiple studies have expanded the definition (see eq 3) as operationally defined by Poulton and Canfield (2005). This detailed speciation approach, as presented in the following Case Study, further refines our understanding of the $Fe_{HR}/Fe_T$ and $Fe_{py}/Fe_{HR}$ threshold values for distinguishing among oxic, ferruginous, and sulfidic bottom waters and specifically demonstrates the influence of magnetite on $Fe_{HR}$ measurements.

The Friends of Anoxic Mud (FOAM) site in Long Island Sound, USA, is an oxic setting with porewater sulfide concentrations as high as 6 mM. Crystalline Fe oxides ($Fe_{ox}$) in FOAM sediments (fig. 3) are most abundant above the zone of sulfide accumulation and then decrease rapidly down core (Canfield, 1989; Canfield and others, 1992; Hardisty and others, 2018). This trend reflects the expected consumption of $Fe_{ox}$ and is similar to other oxic sites with sulfidic porewaters, such as the margin of the Black Sea (Wisjman and others, 2001). FOAM sediments, however, have

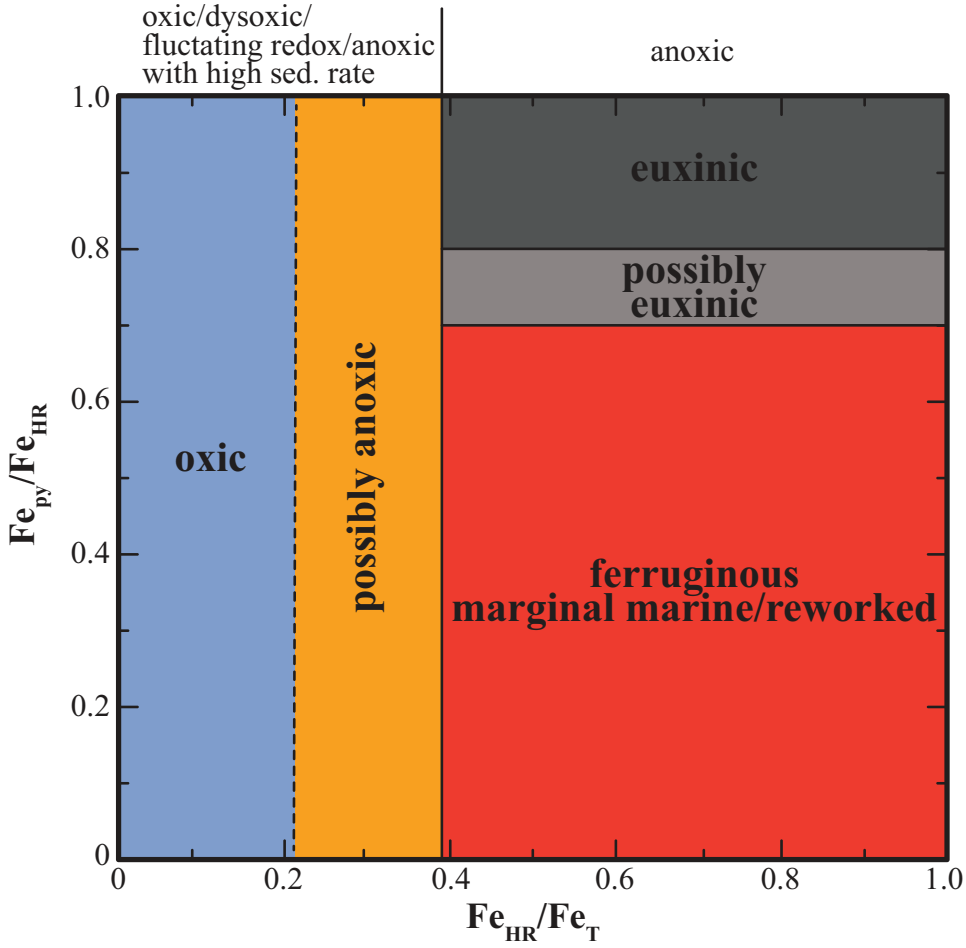


Fig. 2. Diagnostic fields of $Fe_{py}/Fe_{HR}$ and $Fe_{HR}/Fe_T$. Solid lines are recommended values and dashed line is a suggested boundary for ancient sediments only.

$Fe_{HR}/Fe_T$ ratios <0.38 (Raiswell and Canfield, 1998; Hardisty and others, 2018), consistent with their deposition under oxic conditions as is also indicated by $Fe_T/Al$ ratios with values ~0.50 (fig. 3; see also Krishnaswami and others, 1984; Hardisty and others, 2018). In contrast, $Fe_{py}/Fe_{HR}$ ratios at FOAM exceed 0.80 and approach 1, consistent with porewater sulfide accumulation and the near complete conversion of $Fe_{HR}$ to pyrite in these relatively organic C-rich sediments (fig. 3). Similar relationships may occur in other continental margin sediments with high porewater sulfide. However these sites can be distinguished from euxinic waters by considering $Fe_{py}/Fe_{HR}$ ratios in conjunction with $Fe_{HR}/Fe_T$ ratios.

The original data from FOAM used only $Fe_{py}$ and $Fe_{ox}$ to define the highly reactive pool and yielded a $Fe_{HR}/Fe_T$ ratio of 0.20 to 0.30 and $Fe_{py}/Fe_{HR}$ values >0.90 (and approaching 1) within the zone of sulfide accumulation (Raiswell and Canfield, 1998; Hardisty and others, 2018). In the case of FOAM, more detailed speciation based on recent measurements of $Fe_{py}$, $Fe_{ox}$, and $Fe_{mag}$ produces little change in the ratios, with the new values of $Fe_{HR}/Fe_T$ = 0.20-0.30 and $Fe_{py}/Fe_{HR}$= 0.80 to 1.0, suggesting that

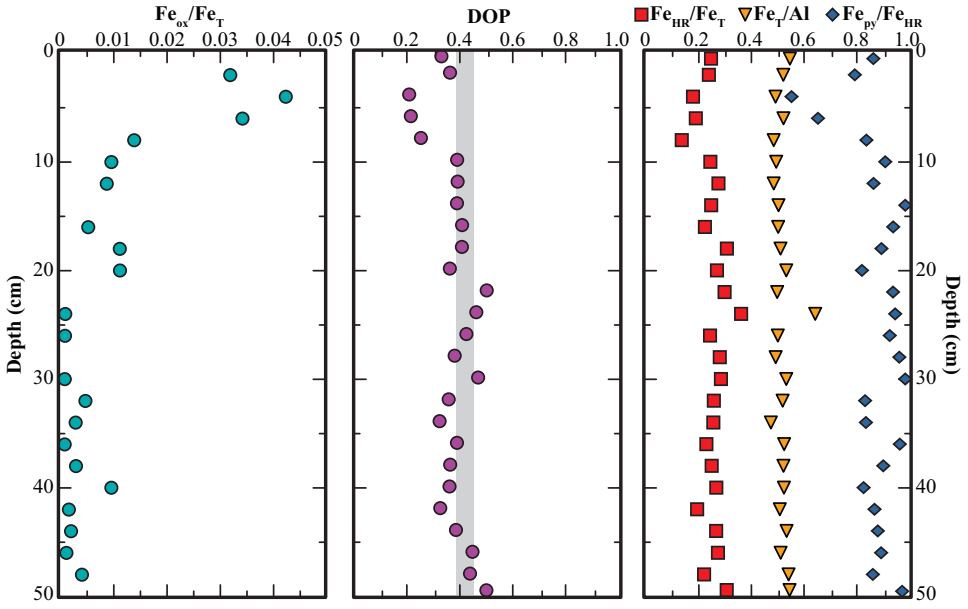


Fig. 3. FOAM porewater and sediment variations with depth (Hardisty and others, 2018). $Fe_{ox}$ represents dithionite-soluble Fe. DOP values are similar to those previously reported at FOAM (Canfield and others, 1992). DOP values below the gray boundary define oxic conditions as do values of $Fe_{HR}/Fe_T$ <0.38 and $Fe_T/Al$ ~0.55 (table 3). Sulfidic pore waters commonly produce values of $Fe_{py}/Fe_{HR}$ >0.8.

the contributions of $Fe_{mag}$ to $Fe_{HR}$ are insignificant. However, in other continental margin sediments, with fundamentally different sediment sources, the inclusion of magnetite in $Fe_{HR}$ might produce a significant decrease in ratios for $Fe_{py}/Fe_{HR}$, which could be particularly important for values that are near the ferruginous threshold.

For example, application of an adapted Poulton and Canfield (2005) sequential extraction scheme to glacially derived non-sulfidic sediments (März and others, 2012), sulfide-limited continental margin sediments (Goldberg and others, 2012), and Baltic Sea sediments with fluctuating redox states (Hardisty and others, 2016) show $Fe_{mag}$ representing a significant fraction of the highly reactive Fe pool. In the case of the glacially derived sediments, $Fe_{mag}$ comprises 0.10 to 0.52 percent of the dry sediment weight in a highly reactive iron pool of 1 to 3 percent (März and others, 2012). From this, we acknowledge the potential for $Fe_{mag}$ to be an important fraction of the highly reactive Fe pool that can potentially affect $Fe_{py}/Fe_{HR}$ and $Fe_{HR}/Fe_{T.}$

The addition of $Fe_{mag}$ and $Fe_{carb}$ is expected to be most important for the recognition of ferruginous environments. Examinations of modern ferruginous marine settings (for example the Orca Basin chemocline) via Fe paleoredox proxies are few in number because of the rarity of this condition in the modern ocean (Hurtgen and others, 1999; Lyons and Severmann, 2006; Scholz and others, 2014a, 2014b), but common ferruginous settings have been inferred from detailed Fe speciation in the geologic past (for example, Poulton and Canfield, 2011; Planavsky and others, 2011; Sperling and others, 2015). Sperling and others (2015) presented a literature compilation of detailed Fe speciation spanning 2300 to 360 million years ago, in which ~3270 data points each include $Fe_{py}$, $Fe_{ox}$ and $Fe_{carb}$. A filtering of a subset of these data for $Fe_{HR}$ <0.40 (as defined by $Fe_{py} + Fe_{ox}$) reveals the potential for major differences for the same data set when highly reactive Fe is defined by the sum of pyrite, dithionite, oxalate, and sodium acetate Fe (compare figs. 4A and 4B). The implication of this

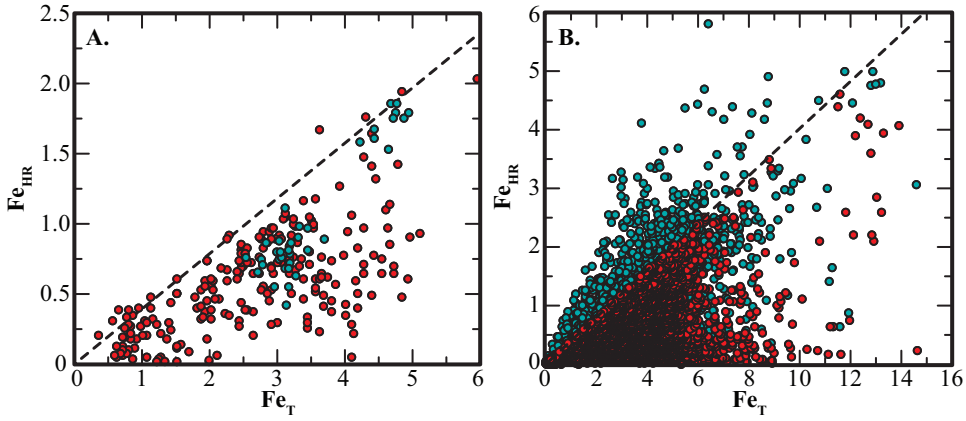


Fig. 4. (A) Compilation of $Fe_{HR}$ versus total Fe for modern oxic marine basins. Red circles indicate studies where $Fe_{HR}$ is the sum of pyrite Fe and dithionite Fe (Raiswell and Canfield, 1998; Wisjman and others, 2001). Green circles represent studies where $Fe_{HR}$ is the sum of pyrite Fe, dithionite Fe and oxalate Fe (Goldberg and others, 2012; Hardisty and others, 2018). The dashed line has a slope of 0.38 which is that found to constrain oxic modern marine basins in previous studies (Raiswell and Canfield, 1998). (B) Compilation of $Fe_{HR}$ versus total Fe for a literature compilation spanning from 2300 to 360 million years ago (Sperling and others, 2015). Red circles represent samples with $Fe_{HR}/Fe_T < 0.38$ with $Fe_{HR}$ measured as the sum of pyrite Fe and dithionite Fe (excluding $Fe_{mag}$ and $Fe_{carb}$ following Raiswell and Canfield, 1998). Green circles show the higher $Fe_{HR}$ data obtained for the same samples where $Fe_{HR}$ is the sum of pyrite Fe, dithionite Fe and oxalate Fe (as proposed by Poulton and Canfield, 2005). The differences between the red and green circles shows how the differences in speciation methodology affect interpretation of the $Fe_{HR}/Fe_T$ threshold.

comparison is that some sediments require measurement of the larger highly reactive Fe suite in order to indicate deposition beneath anoxic bottom waters. The lack of $Fe_{ox}$ and $Fe_{carb}$ measurements may give falsely low $Fe_{HR}/Fe_T$ values (indicating an absence of anoxicity), specifically for sediments deposited beneath ferruginous bottom waters—where there is greater capacity for magnetite (including later overprints), and Fe-carbonates to form and be preserved.

In conclusion, we stress that these threshold values, though proven as useful redox indicators, should be viewed as guidelines and that the full suite of speciation data can be essential. Applications of the updated sequential extraction scheme to modern marine sediments are scarce, with data still lacking for sediments from modern dysoxic, euxinic, fluctuating anoxic or euxinic, and deep sea settings. Considering the small number of modern settings with full sequential Fe data and the importance of factors such as sedimentation rate, threshold values for $Fe_{HR}/Fe_T$ and $Fe_{py}/Fe_{HR}$ should be interpreted cautiously alongside complementary geochemical and paleontological data.

## Case Study 2: Recognizing Depositional Iron Enrichments

Recognition of iron enrichment underpins the $Fe_{HR}/Fe_T$ and $Fe_T/Al$ threshold values that distinguish between oxic and anoxic depositional environments. Correct interpretation of the threshold values requires an understanding of the mechanisms of iron enrichment, which vary among different depositional environments. Enrichment may occur at the time of deposition via the transport of iron from the shelf to a euxinic deep basin, by diagenetic iron mobilization at sedimentological/geochemical boundaries, by detrital sediment delivery, or by upwelling of deep water Fe(II) sourced from hydrothermal vents or porewaters. These examples are discussed below.

*The Black Sea*

The Black Sea is the world's largest modern euxinic basin, with a pycnocline facilitating redox stratification characterized by an oxic shelf and euxinic conditions from the shelf margin to the deep basin. Rapidly deposited sediments occur along the upper slope, where deposition rates range from 0.77 cm/yr or are even instantaneous in the case of turbidites (Crusius and Anderson, 1991; Anderson and others, 1994), and enhanced siliciclastic inputs mute the flux of water column-derived iron—in contrast to the deep basin abyssal plain where sedimentation rates are 0.02 cm/yr (Rozanov and others, 1974; reviewed in Lyons and Berner, 1992). According to current models, iron enrichments in the deep basinal euxinic sediments reflect microbial Fe reduction on the oxic shelf, diffusion of reduced iron into the overlying waters, followed by transport of a proportion of the resulting iron to the deep basin, where it is captured by the sulfidic water column and precipitated as pyrite. The operation of this 'iron shuttle' (see Appendix) allows the accumulation of $Fe_{HR}$ in euxinic settings (Wijsman and others, 2001; Raiswell and Anderson, 2005; Lyons and Severmann, 2006; Severmann and others, 2008, 2010).

Important details have emerged from careful consideration of DOP values in different Black Sea depositional environments. Rapidly depositing muds beneath a sulfidic water column along the basin margin reveal DOP values of ~0.40 (Lyons and Berner, 1992; Canfield and others, 1996; Lyons, 1997; Wijsman and others, 2001; Lyons and Severmann, 2006), $Fe_{HR}/Fe_T$ <0.38 (Wisjman and others, 2001), and $Fe_T/Al$ ratios of ~0.50 (Lyons and Severmann, 2006)—similar to the Black Sea shelf where bottom waters are well-oxygenated (Wijsman and others, 2001) and to other oxic sites like FOAM in Long Island Sound (Goldhaber and others, 1977; Canfield and others, 1992; Raiswell and Canfield, 1998; Hardisty and others, 2018). By contrast, the deep euxinic basin of the Black Sea displays DOP values frequently >0.70 (Lyons and Berner, 1992; Canfield and others, 1996; Lyons, 1997; Wijsman and others, 2001; Lyons and Severmann, 2006), $Fe_{HR}/Fe_T$ >0.38 (Wijsman and others, 2001), and $Fe_T/Al$ ratios of ~0.60 (Lyons and Severmann, 2006), which together with $Fe_{py}/Fe_{HR}$ >0.80, are a euxinic fingerprint. The contrasting dampening of DOP and $Fe_{HR}/Fe_T$, and $Fe_T/Al$ ratios in turbidites and slope settings of rapid deposition is tied to the balance of siliciclastic versus $Fe_{HR}$ input, where relatively high rates of siliciclastic deposition mute the $Fe_{HR}$ enrichment from the shuttle and are thus unfavorable for expression of an anoxic fingerprint, regardless of the redox conditions during deposition. Pyritization of the remaining detrital iron only produces spurious proxy values that are comparable to continental margin sediments, like FOAM (see above). The importance of considering the depositional influences on proxies emerges powerfully from figure 5, where there is a clear inverse relationship between $Fe_T/Al$ and siliciclastic accumulation rates (Lyons and Severmann, 2006).

The non-detrital $Fe_{HR}$ input to anoxic settings is regulated by a shelf-to-basin shuttle and has been studied in detail in the Black Sea (Canfield and others, 1996; Lyons and Severmann, 2006; Severmann and others, 2008). Most of the iron diffusing into the overlying waters on the oxic shelf is rapidly oxidized and re-deposited to surface sediments on the shelf but eventually escapes from the shelf despite many reduction-oxidation cycles (Lyons and Severmann, 2006). Escape creates a deficit of highly reactive iron on the shelf (Wijsman and others, 2001; Lyons and Severmann, 2006; Severmann and others, 2010) that is also revealed by depletions in the lighter Fe isotope on the oxic shelf compared to the input from detrital weathering and the sediments in the deep euxinic basin (Severmann and others, 2008). The implication is that some isotopically light iron produced during microbial iron reduction on the shelf has been exported from that location and accumulates in the deep basin.

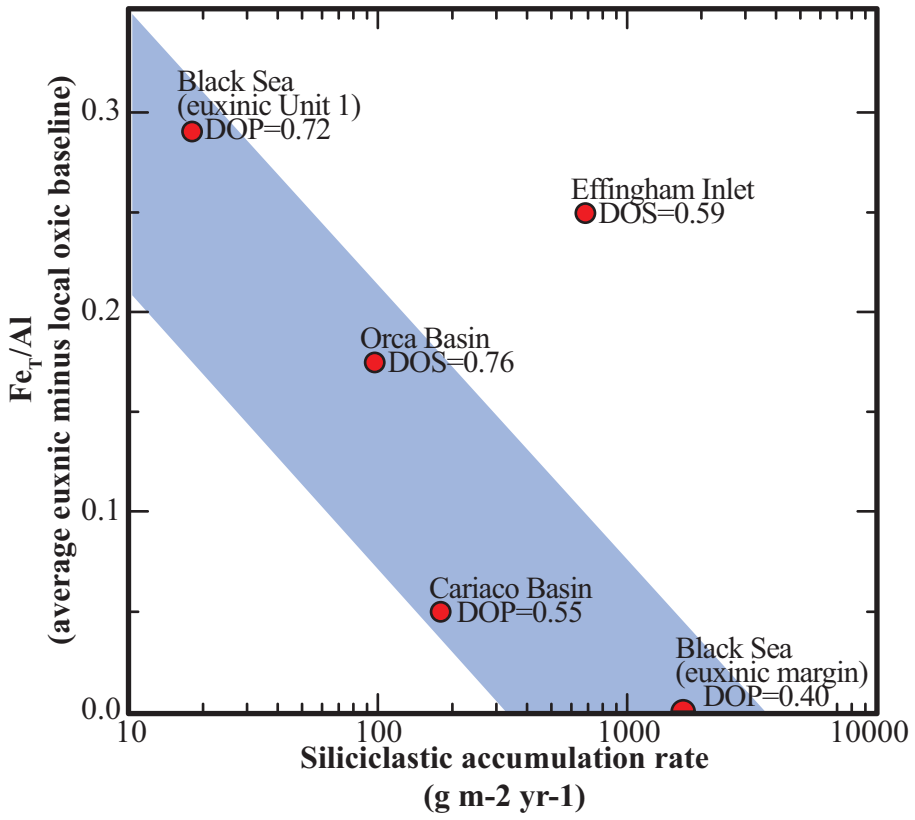


Fig. 5. Dilution effect of siliciclastic accumulation rates on $Fe_T/Al$ (from Lyons and Severmann, 2006).

The Black Sea shows us that iron enrichment in euxinic sediments depends on the amount of $Fe_{HR}$ added to the sediments versus the amount of siliciclastic material. Enhanced delivery of Fe produces an enrichment that can be observed in high $Fe_T/Al$ and $Fe_{HR}/Fe_T$ ratios, in parallel with the high DOP and $Fe_{py}/Fe_{HR}$ values that reflect the ubiquity of sulfide in the euxinic system.

*The Orca Basin*

The Orca Basin is a 400 $km^2$ depression, on the continental slope of the northwest Gulf of Mexico, produced by salt tectonics. Water depths at the basin rim are ~1800 m, increasing to more than 2400 m within the basin. A brine pool occupies the bottom 200 m of the basin, and the strong density gradient limits physical exchange between the brine and overlying seawater. Dissolved oxygen is rapidly depleted at 2200 m depth, and the brine below that depth is permanently anoxic, with ferruginous conditions at the pycnocline and euxinia in the deepest waters. A large fraction of the particulates settling into the basin are trapped along a sharp density interface, producing a dramatic rise in particulate Fe at the brine/redox interface (Trefry and others, 1984; Van Cappellen and others, 1998).

Lyons and Severmann (2006) studied sites on the oxic margin and within the adjacent anoxic basin, as well as in the intermediate, chemocline portion of the water column. They reported data for HCl-soluble iron, sulfidic iron (both pyrite and AVS), $Fe_T$, and Al. Sediments on the oxic margin consist of homogenous, bioturbated

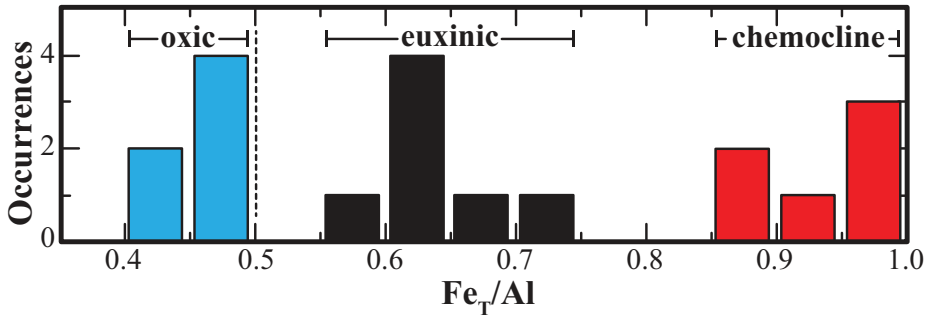


Fig. 6. $Fe_T/Al$ ratios for Orca Basin sediments (from Lyons and Severmann, 2006). Dashed line represents mean ratio in modern sediments (see table 3).

olive-brown to light gray muds with Fe sulfide levels falling below the detection limit. By contrast, sediments within the anoxic basin are soupy, black laminated muds containing ~1 percent AVS and ~0.1 percent pyrite S.

DOS values in the Orca Basin sediments below the chemocline range from 0.40 to 1.0 (Lyons and Severmann, 2006). Sediments within the chemocline at 2240 m are brick red with gray mottling, and the sulfide contents here are also below detection limits, resulting in near-zero DOS values. Iron enrichment in the chemocline is clearly not the result of sulfide precipitation but instead is produced by the deposition of iron (oxyhydr)oxides where the particulate iron maximum impinges on the seafloor. This particulate iron (oxyhydr)oxide maximum is sourced by the oxidation of reduced iron supplied from the underlying anoxic waters to the oxic-anoxic boundary at the chemocline. Lyons and Severmann (2006) noted that the iron enrichments in the chemocline are not expressed in elevated DOS values. No dithionite data were reported, but the absence of sulfides requires $Fe_{py}/Fe_{HR}$ to be near-zero. Total iron extraction does, however, produce elevated $Fe_T/Al$ values (fig. 6). Together, the low DOS and enriched $Fe_T/Al$ (and presumably high $Fe_{HR}/Fe_T$ and low $Fe_{py}/Fe_{HR}$) specifically identify a ferruginous setting at the pycnocline, consistent with water column observations of redox zonation within the Orca Basin (Van Cappellen and others, 1998).

### *The Peruvian Oxygen Minimum Zone (OMZ)*

Similar to the Orca Basin chemocline, enriched values of $Fe_T/Al$ have been noted along the oxic-anoxic boundary of the Peruvian OMZ (Scholz and others, 2014a, 2014b), where dissolved Fe accumulates in the waters but dissolved sulfide is absent (Chever and others, 2015). In this case, however, it was specifically observed that $Fe_T/Al$ and Fe isotopes within the core of the Peruvian OMZ, where conditions are most reducing, did not reflect an anoxic setting. Instead, these values were similar to those of the oxic shelf of the Black Sea, indicating that the sediments and water column in the low oxygen setting similarly remobilize and transport $Fe_{HR}$ to environments more favorable for deposition—in this case the anoxic-oxic boundary (Scholz and others, 2014a, 2014b). $Fe_{HR}/Fe_T$ and $Fe_{py}/Fe_{HR}$ were further evaluated as part of the study (using $Fe_{HR} = Fe_{ox} + Fe_{py}$), revealing elevated values near or at the previously discussed 'thresholds' for euxinic water column at the OMZ anoxic-oxic boundary. Water column sulfide accumulation was not noted. These indications of euxinia may be a function of missing $Fe_{HR}$ fractions, which would otherwise yield the appropriate ferruginous signal (see Case Study 1). Large concentrations of glauconite (up to 15 wt. %) are being produced from $Fe_{HR}$ fractions due to the oscillatory nature of the

fringes of the OMZ. Glauconite (with both ferric and ferrous Fe) is essentially insoluble in dithionite (Raiswell and others, 1994), and failure to account for this source of $Fe_{HR}$ produces a falsely high $Fe_{py}/Fe_{HR}$ signal for euxinia. Alternatively, similar to the diagenetic remobilization scenarios discussed as part of Case Study 3, exposure of the 'highly reactive' Fe to porewater sulfide at the fringes of the OMZ may promote diagenetic pyritization of the $Fe_{HR}$ pool, leading to a false euxinic signal. Regardless, these scenarios have the potential to produce false euxinic signals for the oxic-anoxic (ferruginous) transition if Fe proxies are used alone. We stress that such settings can be distinguished in the geologic record, as they lack the Mo enrichments typical of euxinia.

### *Quaternary Glacial Sediments*

Depositional iron enrichments have also been documented in sediments from glacial-interglacial cycles in the Quaternary Arctic (März and others, 2012). The Central Arctic Ocean contains prominent, basin-wide brown layers enriched in Mn and Fe (oxyhydr)oxides that occur during interglacial intervals. These horizons show high values of $Fe_T/Al$ (up to 0.68) that are typical of euxinic or ferruginous conditions. However, the mean values of $Fe_T/Al$ are 0.59 in both the glacial and interglacial intervals, which suggest a high local baseline. There is a near-complete lack of pyrite in these organic-poor sediments ($Fe_{py}/Fe_{HR}$ is $<0.05$), and thus DOP is low, and euxinia would not be predicted. The $Fe_{HR}/Fe_T$ ratio in the interglacial intervals (0.45–0.60) lies above the oxic/anoxic threshold, but the $Fe_T/Al$ data are $<0.66$. The $Fe_{HR}/Fe_T$ data suggest a ferruginous depositional environment that requires further investigation via the geochemical, sedimentological, and paleoceanographic context.

The interglacial intervals correspond to decreases in Al and $Fe_T$, which suggest an important sedimentological/provenance control (März and others, 2012). High baseline $Fe_T/Al$ may be partially responsible for the apparently ferruginous $Fe_T/Al$ values, but März and others (2012) also suggest that the peaks have been blurred by post-depositional migration of Fe from anoxic porewaters up to the sediment surface where Fe (oxyhydr)oxides are precipitated. This mechanism requires oxic bottom waters. The proxy data in this sequence suggest anoxic bottom waters, but crucially, there is no paleoceanographic evidence for widespread ferruginous bottom waters in the Arctic during the last 13,000 yr. Thus, März and others (2012) show that the interglacial periods produced enhanced transport of $Fe_{HR}$ from the Arctic rivers and into the deep basin, coupled with early diagenetic enrichment of Fe and Mn at the sediment/water interface. Here, resolution of ambiguous proxy signals has ultimately been possible only because an oceanographic context is available for recent sediments.

## CASE STUDY 3: RECOGNIZING DIAGENETIC IRON ENRICHMENTS

Cases of diagenetic remobilization and enrichment may also be difficult to recognize from proxy data alone but should be considered wherever there is a juxtaposition of sediments with compositions that have different potentials for diagenetic reactions involving organic C, sulfur, and iron. Berner (1969) designed experiments to study the diagenetic behavior of organic C-rich layers enclosed by organic C-poor sediment. Three different cases were recognized based on the relative amounts of reactive Fe and dissolved sulfide—described as having high, low, or intermediate Fe contents, which determined whether sulfide or iron diffused into the organic C-rich sediments. The addition of sulfide or iron from the surrounding sediments potentially confounds the use of iron proxy data to determine the depositional environments of the organic C-rich horizon and the surrounding organic C-poor sediments.

The high $Fe_{HR}$ model was arbitrarily defined by Berner (1969) as applying to organic C-rich sediments generating sulfide but with a high enough $Fe_{HR}$ content to maintain sulfide at low levels. Dissolved iron in the organic C-poor sediments below

(or from the water column above) can then diffuse to the base of, or into, the organic C-rich layer to form pyrite. The addition of Fe (which is fixed by sulfide) may be sufficient to produce signatures of euxinia in the organic C-rich layer.

The low reactive Fe model of Berner (1969) occurs where sulfate reduction produces sufficient sulfide to consume all the $Fe_{HR}$ within the organic C-rich layer. Sulfide then diffuses downwards into the organic C-poor sediment, where it forms pyrite at the edges of the lithological transition using $Fe_{HR}$ contained within the sediment and porewater Fe along the migration pathway. Sulfide migration alone is the key signature for this model. In the absence of iron enrichment within the organic-rich layer, the original oxic sediment signatures of the organic C-poor sediments would remain unaltered, but $Fe_{py}/Fe_{HR}$ may approach euxinic levels. The association of oxic $Fe_{HR}/Fe_T$ values with high $Fe_{py}/Fe_{HR}$ is inconsistent with euxinia and indicates that porewaters were Fe-limited during diagenetic pyrite formation. In this case, the influence of migration can be recognized because the high $Fe_{py}/Fe_{HR}$ values cross a prominent lithological boundary and because oxic values are still recorded by $Fe_{HR}/Fe_T$, $Fe_T/Al$, and DOP (see also Owens and others, 2012).

### *The Mediterranean Sapropels*

At intermediate reactive iron contents, dissolved sulfide migrates downwards from an organic C-rich layer into an organic C-poor layer where it meets upward diffusing Fe (Berner, 1969). The depth of pyrite formation then depends on the relative rates of supply of sulfide and dissolved Fe. This model has been used to explain the migration (and enrichment) of both Fe and sulfide in the Mediterranean sapropels, where deposition of organic C-rich sapropels occurs within a thick sequence of organic C-poor sediments. Unfortunately, there are no $Fe_{HR}$ data for the sapropels, but Passier and others (1996) show that the organic C-rich sapropel layer ($S_1$ in core GC17) is enriched in organic C (2–3%), pyrite sulfur (~1%), and Fe (the $Fe_T/Al$ ratio is ~0.70), which is consistent with an euxinic origin (fig. 7). The sediments about 5 cm below the sapropel have essentially the same compositions, but the sediments 15 cm below have lower organic C contents (<0.3%), lower S contents (~0.1%), and $Fe_T/Al$ ~0.50, consistent with deposition under oxic conditions.

Passier and others (1996) interpret the sapropel to have either been deposited under sulfidic bottom waters or to have produced sufficient sulfide to consume all the $Fe_{HR}$ and generate sulfidic porewaters. Sulfide then diffused downwards into the organic C-poor sediment immediately below to produce enrichment in pyrite sulfur (fig. 7). However the sediment below the sapropel (depths ~0.25–0.30 mbsf) is also enriched in $Fe_T$ thus producing $Fe_T/Al$ ratios comparable to those in the sapropel and much higher than in the sulfide-poor sediments below 0.3 mbsf. Hence, pyrite has formed using $Fe_{HR}$ contained within the sediment plus dissolved iron diffusing upwards that is liberated from $Fe_{HR}$ in sediments lower in the sequence. Migration of Fe upwards to this horizon has to occur to produce the observed elevated $Fe_T/Al$ values in the organic-poor sediments that were deposited beneath oxic bottom waters. This migration of Fe confounds the use of the Fe proxies, as the horizon below the sapropel now contains proxy signals that have been altered by the addition of $Fe_{HR}$ to yield $Fe_T/Al > 0.55$ (and likely $Fe_{HR}/Fe_T > 0.38$, and $Fe_{py}/Fe_{HR}$ ratios of 0.80–1.0). These signals are consistent with euxinia, in clear contradiction with the depositional environment, but the influence of migration can be recognized in this case because the high proxy values persist across the prominent lithological boundary between the organic C-rich and organic C-poor sediments. The sedimentological context provides key insight.

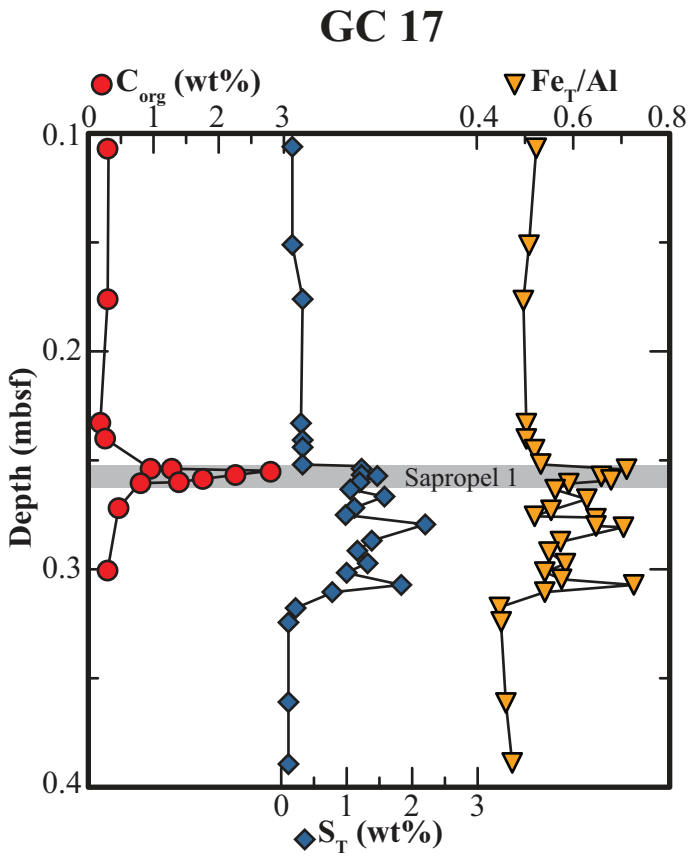


Fig. 7. Depth variations in organic C, total S and $Fe_T/Al$ for sapropel S1 in core GC17 (from Passier and others, 1996). Enrichments in pyrite S and $Fe_T/Al$ are found within the sapropel and in the sediments below.

*The Baltic Sea*

The Baltic Sea represents a unique depositional setting where, ~8 to 8.5 kyr ago, rising sea level transitioned the Baltic basin from a freshwater lake to the modern brackish conditions. This transition is recognized throughout the basin by changes in faunal communities and sedimentology, as well as a change from low to high organic C contents (Andrén and others, 2011). Directly following this salinity transition, the ensuing silled basin formed a halocline, resulting in an anoxic period lasting ~4 kyr and recognized in multiple sub-basins in the Baltic Sea by lamination records (Zillén and others, 2008). In line with these relationships, multiple geochemical records show elevated DOP (and DOS), $Fe_T/Al$, $Fe_{HR}/Fe_T$, $Fe_{py}/Fe_T$, and trace metals indicative of a euxinic water column in some sub-basins, all coincident with increases in organic C >4 weight percent (Boesen and Postma, 1988; Sohlenius and others, 1996, 2001; Lepland and Stevens, 1998; Fehr and others, 2008; Jilbert and Slomp, 2013; Hardisty and others, 2016). The Baltic sediments have a particularly high abundance of AVS that requires the use of the Degree of Sulfidation and $(Fe_{py} + Fe_{AVS})/Fe_{HR}$, which is preferred (see earlier) over DOP and $Fe_{py}/Fe_{HR}$ for euxinic systems when AVS is present in appreciable amounts.

In the lacustrine, organic C-poor clay sediments directly underlying the brackish muds, multiple studies have observed the mobilization of sulfate and sulfide downwards

from the overlying brackish sediments, as in Berner's low Fe model. In this case, unlike the intermediate Fe model, upward fluxes of porewater Fe from the lacustrine sediments constrain downward dissolved sulfide migration, and hence post-depositional $Fe_{HR}$ and $Fe_{py}$ enrichments occur directly along the margins of the sediment transition. As a result, Fe enrichment produces elevated $Fe_T/Al$ and DOS as well as $Fe_{HR}/Fe_T$. Multiple studies have noted enrichments of pyrite, Fe monosulfides, greigite, and elemental S in the lacustrine sediments directly underlying the brackish sapropel (for example Boesen and Postma, 1988; Holmkvist and others, 2014). Reported DOS values in these lacustrine sediments are typically near 0.4, elevated from a baseline of DOS ~0 through post-depositional enrichment (Boesen and Postma, 1988). DOS ~0.4 is consistent with an oxic setting and indicates that sulfidation of the *in situ* $Fe_{HR}$ pool is more important than addition from upward diffusing dissolved Fe, thus preventing false anoxic signals in these cases.

### *Sulfur Isotope Signals of Fe Enrichment*

Iron enrichments in the Mediterranean sapropels and the Baltic Sea are recognized by multiple, elevated proxy values that occur across prominent sedimentological boundaries. These circumstances in the Recent and Phanerozic record can often be identified by sulfur isotope data even with limited other proxy data. The early stages of sulfate reduction are characterized by the production of isotopically light sulfide (typically $\delta^{34}S$ $<-40$ to $-20‰$). Continued sulfate reduction produces heavier dissolved sulfide, which can diffuse away to form pyrite with relatively heavy isotopic values in adjacent sediments. Middelburg (1991) demonstrated iron enrichment across a marine-freshwater boundary in Kau Bay (Indonesia) using sulfur isotope data. Here, marine sediments are being deposited from bottom waters that are commonly low in oxygen and non-sulfidic but intermittently euxinic. In the past, the basin became isolated from the ocean and brackish/freshwater sediments were deposited. There are only two samples from the brackish/freshwater sediments, and proxy data are limited. Nevertheless, Middelburg (1991) showed that the marine, brackish and freshwater sediments have rather similar organic C contents (3–5%), but the freshwater sediments are enriched in sulfide sulfur, which is isotopically heavier ($\delta^{34}S$ up to $+15‰$) than the overlying marine sediments ($\delta^{34}S$ $-24$ to $-17‰$). Isotopically heavy sulfides also occur across lithological boundaries in the Cariaco Basin (Lyons and others, 2003) as well as in the freshwater sediments of the Black Sea (Jorgensen and others, 2004), where methane diffuses upward into iron-rich sediments and drives sulfate reduction to produce an isotopically heavy sulfidiation front ($\delta^{34}S$ +15 to $+34‰$).

In conclusion we note that diagenetic iron enrichments are driven by depositional and associated geochemical discontinuities (non-steady state conditions), and all these cases require careful consideration of proxy data in relation to their geochemical and sedimentological context and the depositional environment more generally. Interpreting ratio changes at facies/lithological boundaries requires extreme caution.

## Case Study 4: Recognizing Enrichment Processes with Mo Abundances and Fe Isotopes

Case Studies 2 and 3 explored mechanisms of localized iron enrichment in marginal basins and epicontinental seas, as these have been the focus of many previous studies using the iron proxies. However, multiple enrichment processes may operate on an ocean-wide scale where signals from localized processes may occur together with basin-wide processes. Resolving complex, mixed signals, requires additional evidence from other geochemical proxies, as well as careful consideration of the geological context.

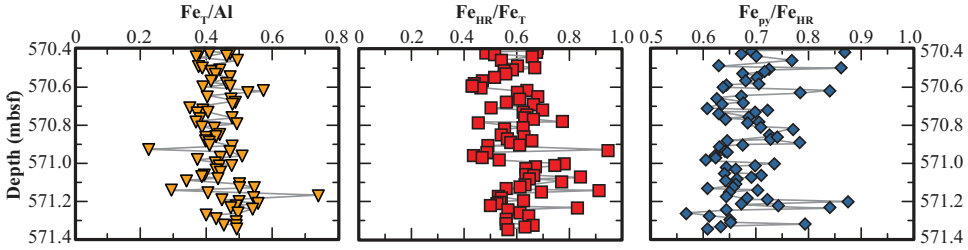


Fig. 8. Variations in the iron proxies ($Fe_T/Al$, $Fe_{HR}/Fe_T$ and $Fe_{py}/Fe_{HR}$) through core at site 1261 (from März and others, 2008). $Fe_{HR}/Fe_T$ values >0.38 indicate Fe-enrichment, values of $Fe_{py}/Fe_{HR}$ >0.70 are possibly euxinic.

*Cretaceous Black Shales with Shuttle and Hydrothermal Fe Sources*

This example considers the geochemical signatures of ferruginous or sulfidic bottom waters in an oceanic depositional environment where there is potential for hydrothermal activity. This case study (from März and others, 2008) is based on a core retrieved during ODP Leg 207 at site 1261 on the Demerara Rise in the equatorial Atlantic. The sediments consist of a finely laminated black claystone that spans the Cretaceous Oceanic Anoxic Event (OAE 3). OAE 3 corresponds with a period of enhanced hydrothermal activity (Jones and Jenkyns, 2001) and thus, the possibility that hydrothermal fluxes would have reached the Demerara Rise at this time cannot be ignored.

The core was analyzed for $Fe_T$, Al, and inorganic C, with iron speciation carried out by sequential extractions to quantify $Fe_{carb}$, $Fe_{ox}$, $Fe_{mag}$, and $Fe_{py}$, the sum of which defines $Fe_{HR}$. The calcium carbonate ($CaCO_3$) content is typically ~60 percent and rarely exceeds 80 percent, $Fe_T$ contents average ~1 percent (only one sample contains <0.5%,) and organic C contents are always >2 percent. These compositions allow use of the iron proxies (see table 3). The $Fe_{HR}/Fe_T$ ratios mostly lie between 0.40 and 0.65 except for a few intervals where $Fe_{HR}/Fe_T$>0.80, and thus iron enrichment is clearly indicated (fig. 8). Further detail emerges by considering the $Fe_{py}/Fe_{HR}$ data, which vary between approximately 0.60 and 0.90, with many values lying above 0.70 (in the range of possible euxinia), but only five samples have $Fe_{py}/Fe_{HR}$>0.80 (and give clear euxinic signals). None of these five has a $Fe_T/Al$ ratio >0.60, but figure 8 shows that $Fe_T/Al$ frequently lies below 0.50, which suggests that the local threshold for $Fe_T/Al$ enrichment is significantly below 0.55. These subdued $Fe_T/Al$ signals are inconclusive evidence for euxinia but the $Fe_{HR}/Fe_T$>0.40 suggests the sequence is generally Fe-enriched and possibly euxinic (when $Fe_{HR}/Fe_T$ >0.70).

However, Mo abundance provides crucial diagnostic evidence (März and others, 2008). The behavior of Mo has been discussed in detail in Scott and others (2008) and Scott and Lyons (2012), among many other papers, and only brief details are supplied here. Molybdenum enrichments exceeding 100 ppm are strong evidence for the presence of hydrogen sulfide and abundant dissolved Mo in the water column. However, enrichments above the crustal average (1–2 ppm) and below 25 ppm indicate that dissolved sulfide was present but only in the porewaters. Concentrations between 25 and 100 ppm are characteristic of oscillatory or seasonal euxinia or restricted systems with persistent euxinia that draw down the Mo reservoir (Scott and Lyons, 2012). März and others (2008) show that the sediments at site 1261 never show Mo <50 ppm, and there are prolonged periods with Mo >100 ppm. These high Mo samples have a mean $Fe_{py}/Fe_{HR}$ of 0.68±0.06, close to the lower limit of 0.70 for euxinicity (table 3). The Mo signals of euxinia clarify the iron proxy signals and

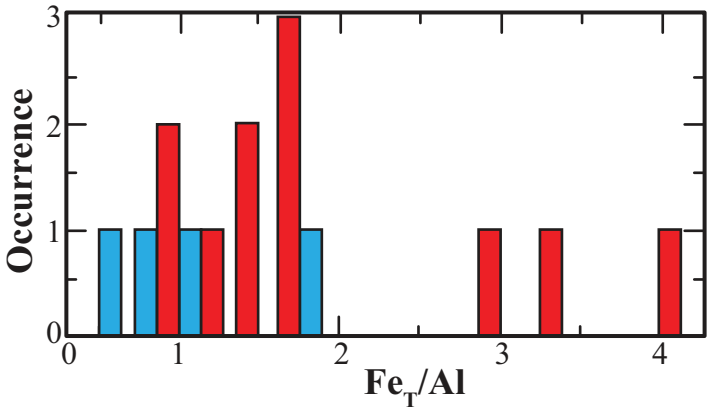


Fig. 9. Maximum $Fe_T/Al$ values in modern (blue) and ancient (red) euxinic sediments (from Raiswell and others, 2011). The two values above 3.0 are from Precambrian sediments (see text).

support the interpretation of März and others (2008) that persistent euxinia was punctuated by brief periods of anoxic, non-sulfidic bottom waters—that latter being recorded in the transitional Fe data. The $Fe_T/Al$ values at this site are $<<2.0$ and are more likely to result from euxinicity than a hydrothermal source (see fig. 9 and earlier). We caution, however, that these Mo relationships can be compromised at time of widespread euxinia when the global marine inventory is drawn down and sediment enrichments in individual euxinic settings are correspondingly muted (for example Scott and others, 2008).

*Cretaceous Black Shales with Multiple Iron Sources*

In this Case Study, we discuss Deep Sea Drilling Project (DSDP) Sites 105, 367, and 144 using data from Owens and others (2012), who explore the causes of iron enrichment in a basin-wide context. In this case several contemporaneous enrichment processes occur to varying degrees, and their relative contributions can only be deciphered by using iron proxy data supported by Mo abundance and iron isotopes. These sediments deposited during OAE 2 record the pervasive deposition of black shales on the continental shelves extending to deep waters.

Deposition at Site 105 is marked by alternating organic-poor, bioturbated green claystone (with organic C ~1%) and black shales (organic C up to 25%) that clearly record fluctuating redox conditions. Site 367 is the deepest and is located near the ancestral mid-ocean ridge. Prior to, and during the OAE, deposition at this site consisted of laminated, organic C-rich sediments (up to 40% organic C) with biomarker evidence that suggests euxinic conditions extended into the photic zone. Site 144 sediments consist of interlayered, laminated carbonaceous limestone and calcareous clays (organic C up to 30%) that were deposited at shallow depths on the mid-ocean ridge. The origin of OAE 2 has been postulated to reflect an expansion of hydrothermal activity that generated iron-rich conditions in the photic zone which stimulated enhanced primary production, even prior to the OAE. However, iron-enriched sediments can also be produced by shuttle delivery and diagenetic remobilization, and Owens and others (2012) sought to distinguish these, and the hydrothermal, signals using $Fe_T/Al$ data supported by Mo abundance and iron isotopes.

Iron isotopes provide additional perspective because specific enrichment mechanisms can have diagnostic isotopic signatures. Hydrothermal iron shows relatively little

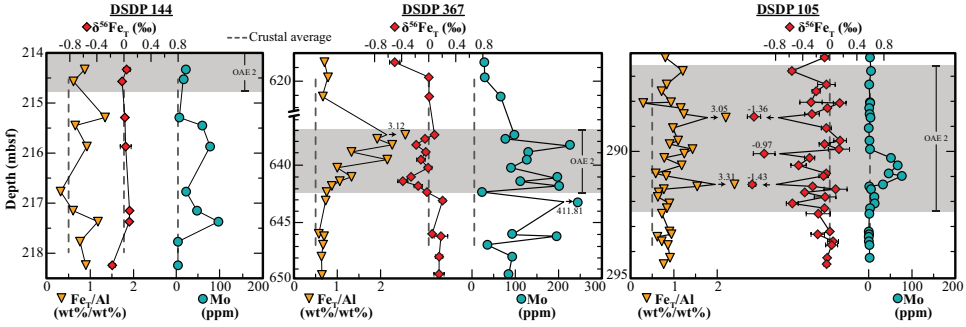


Fig. 10. Stratigraphic variations in $Fe_T/Al$, $\delta^{56}Fe$ and Mo abundance at DSDP sites 367, 144 and 105 (from Owens and others, 2012). Error bars represent precision of 0.08‰. The gray bar shows the location of OAE 2. $Fe_T/Al$ values of 1–2 are Fe-enriched with Mo >100 ppm indicating euxinicity.

deviation in $\delta^{56}Fe$ from average igneous rocks (~0.0 to −0.5‰). However, operation of an iron shuttle requires that high concentrations of porewater Fe are formed by iron reduction, which produces isotopically light dissolved iron that diffuses into the overlying seawater and is transported to basinal areas. Transported iron encountering sulfidic conditions is precipitated, often quantitatively, and the resulting pyrite is isotopically light. Isotopically light pyrite also forms when porewater iron is mobilized and precipitated as pyrite during diagenesis, usually where sediments with very different organic C contents are interlayered (see Case Study 3).

Sediments at Site 144 show high values of $Fe_T/Al$ even before the OAE (fig. 10) but with considerable variability from <0.50 to >1.5. All the Fe isotope data are uniform, with $\delta^{56}Fe$ averaging ~0.0 permil both before and during the OAE. High values of $Fe_T/Al$ with iron isotope data that inversely track the level of enrichment would result from shuttle delivery (Severmann and others, 2008), while the absence of co-variation is more consistent with a hydrothermal source (Owens and others, 2012). The location of Site 367 is an area of pervasive euxinicity (indicated by Mo values >100 ppm and consistent with $Fe_T/Al$ values ~2.0). A hydrothermal contribution is likely at this location but there are weak shifts in $\delta^{56}Fe$ towards negative values that suggest a minor shuttle contribution. However there is no correlation between the shifts in $\delta^{56}Fe$ and $Fe_T/Al$, which should occur if shuttle sources predominated. These contributions must have been minor compared to hydrothermal inputs (Owens and others, 2012). Site 105 shows complex, fluctuating patterns wherein high $Fe_T/Al$ values correspond with very negative $\delta^{56}Fe$ (fig. 10), which would indicate substantial shuttle contributions. However Mo concentrations are mostly <16 ppm, and thus persistent euxinia is unlikely. Instead, the interlayering of organic C-rich and organic C-poor sediments indicates that the variability in Fe enrichments and isotope composition most likely result from diagenetic remobilization (see Case Study 3). These examples from Owens and others (2012) show the value of coupling Mo concentrations with iron isotope and speciation data.

### Case Study 5: Recognizing the Influence of Burial and Metamorphism

The iron proxies have often been applied to ancient sediments, although there is potential for the abundances of Fe and S species to be significantly modified by deep burial or metamorphic fluid processes that add or remove Fe and S or alter their speciation. There are numerous potential reactions that can involve the addition or removal of iron as carbonates, oxides, sulfides, and silicates during burial or metamorphism and special care is therefore needed to avoid false signals in deeply buried and

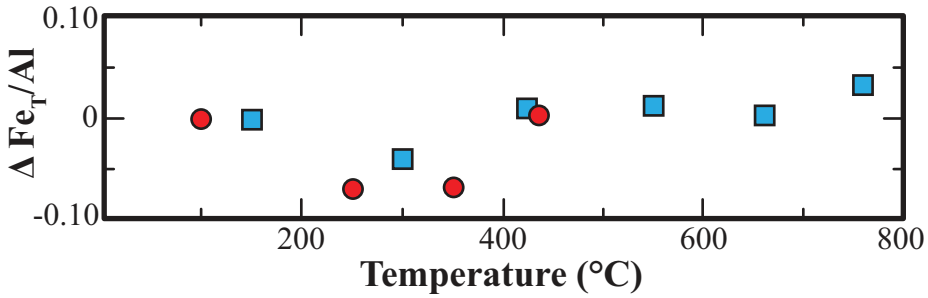


Fig. 11. Δ $Fe_T$/Al variations with temperature (blue squares data from Jia, 2006; red circles data from Yui and others, 2009).

highly metamorphosed sediments (Raiswell and others, 2011; Asael and others, 2013; Reinhard and others, 2013; Slotznick and others, 2018). An important first step is to examine the petrography of samples representative of the major lithologies for any evidence that the sediments were open or closed to fluids that added or removed Fe and S. Addition may be recognized by late overgrowths on diagenetic phases or by the occurrence of new, late-stage minerals. In some cases, it may be possible to use petrographic, trace element or isotopic data to quantify the extent of addition or loss, and the speciation data can then be corrected back to their pre-alteration values (or the samples can be avoided).

The simplest cases will be those where iron is conserved (recognized by uniform $Fe_T$/Al) but transferred among different carbonate or oxide species that contribute to $Fe_{HR}$. A plot of $Fe_T$/Al may provide a preliminary indication of open versus closed system behavior for iron during metamorphism, but caution is needed as secondary overprints might also reflect Fe migration at lithological boundaries or a varying depositional environment. There is also potential for proxy data to be altered where systems are open to the transfer of C-O-S-H species that may alter speciation (Asael and others, 2013; Reinhard and others, 2013; Slotznick and others, 2018). Further, it is also imperative, where possible, to use a local threshold to define iron conservation—as the following example will show. Figure 11 includes $Fe_T$/Al data from Jia (2006) from the Paleozoic Cooma metamorphic complex (SE Australia). At this location, metapelites of uniform age and composition occur across a continuous metamorphic grade from subgreenschist (~150 °C) to upper amphibolite (760 °C) facies. The mean $Fe_T$/Al ratio of the subgreenschist facies sediments is 0.39, which is used as a threshold for local oxic (non-Fe enriched) conditions. Thus, we define Δ $Fe_T$/Al as $(Fe_T/Al)_t$ - $(Fe_T/Al)_l$, where the subscripts *t* and *l*, denote respectively the $Fe_T$/Al ratio for any temperature *t* and for the local $Fe_T$/Al ratio threshold *l*. A set of $Fe_T$ and Al data are also available in Yui and others (2009) over a smaller temperature range (100–435 °C) for pelites of Tertiary age with essentially the same mineral composition and the mean $Fe_T$/Al ratio of the zeolite facies (0.47) is used as a local threshold. Figure 11 reveals little variation in Δ $Fe_T$/Al for both sets of data as a function of temperature, and iron has clearly been conserved in both cases across substantial temperature gradients. Slotznick and others (2018) also found near-conservation of $Fe_T$ across metamorphic grade and hence proxy data from DOP, $Fe_{py}/Fe_{HR}$, $Fe_{HR}/Fe_T$, and $Fe_T$/Al will all remain valid provided there are no speciation changes resulting from the additions of C-O-S-H-bearing fluids.

A more complex case arises where changes in $Fe_T$/Al can be identified. Such changes may occur where the depositional environment changes between oxic and euxinic or where boundary effects produce iron migration (see Case Study 3). These

cases may be recognized by lithological discontinuities and by changes in DOP and careful interpretation of samples in their lithological context may avoid false signals. However the addition or removal of iron by during metamorphism may add or remove Fe from $Fe_{HR}$ and/or $Fe_{py}$ and will produce false signals unless such changes are identified by petrographic or isotopic data.

Changes in both iron and sulfur speciation can arise as a consequence of metamorphic reactions by which pyrite is altered to pyrrhotite (Reinhard and others, 2013; Slotznick and others, 2016). Slotznick and others (2018) found pyrrhotite formation that was a major influence on iron speciation data. In theory, however, proxy data can be corrected by apportioning pyrrhotite into different iron pools, assuming that pyrrohotite Fe can be accurately determined. Asael and others (2013) extracted crystalline pyrrhotite using a hot 6N HCl distillation with $SnCl_2$ acting as a reductant. This method is too aggressive for the complete separation of pyrite from pyrrhotite in modern sediments but in ancient metamorphosed sediments, where pyrite is more crystalline, the relative yields of pyrrhotite and pyrite can be quantified as the difference between chromium reducible sulfur (which extracts both pyrite and pyrrhotite; Canfield and others, 1986) and the sulfur extracted by $HCl/SnCl_2$. Provided pyrrohotite concentrations are low, the cautious interpretation of all chromous chloride-extracted S as pyrite will not introduce major errors.

Large concentrations of pyrrhotite present intractable problems because different pyrrohotite-forming reactions derive iron from different iron pools and thus have different consequences for the iron proxies. Pyrite can be altered to pyrrhotite using $Fe_{HR}$ or Fe from silicates, can be converted to pyrrhotite by the introduction of Fe-bearing fluids, and can be formed by the thermal decomposition of pyrite. These reactions all have different consequences for total sulfur, total iron, $Fe_{HR,}$ and sulfide species and thus for the iron proxies. In theory, determination of pyrrhotite sulfur would allow the pre-alteration rock composition to be derived, *provided the correct reaction can be identified and assuming only one process is involved.* The overarching message is that rocks with significant concentrations of pyrrhotite are best avoided unless Fe speciation can be constrained by petrographic or field observations (Slotznick and others, 2018).

The presence of diagenetic carbonates may also exert a significant effect on the determination of $Fe_{HR}$ (Slotznick and others, 2018). Clarkson and others (2014) found that the ratio $Fe_{HR}/Fe_T$ in modern carbonates with minimal diagenetic overprinting behaves essentially the same as siliciclastic rocks. However deep burial dolomitization using an external source of iron severely compromises proxy data and Clarkson and others (2014) suggested that ankerite-rich samples are best avoided. Slotznick and others (2018) also found that $Fe_{HR}/Fe_T$ signals were potentially compromised by trace amounts of Fe in carbonates that produced false signals for a ferruginous water column. It was concluded that samples with proportionately high $Fe_{carb}$ should be investigated petrographically to determine whether the carbonates are primary or reflect diagenetic/metamorphic processes. The problem essentially relates to the source of iron which may not necessarily be derived from other *in situ* $Fe_{HR}$ phases, and may be derived instead from an external source. Iron from an external source may produce high $Fe_T/Al$ values and such samples with high concentrations of $Fe_{carb}$ should be subjected to further detailed petrographic, microprobe and/or isotopic analysis. We are in full agreement with Slotznick and others (2018) that mineralogical and petrographic approaches should be combined with iron speciation data to disentangle the effects of post-depositional processes on metamorphic rocks – ultimately to provide an accurate picture of paleoenvironmental redox conditions. In sum, proxy data must be used with extreme caution when metamorphic overprints are substantial (Slotznick and others, 2018).

### CASE STUDY 6: PRECAMBRIAN SEDIMENTS: BRINGING IT ALL TOGETHER

Our Case Studies have illuminated a range of potential problems that we now revisit in relation to applications in Precambrian sediments where unique challenges exist for several reasons. First, the absence of fossils makes it impossible to calibrate the thresholds against paleoecological observations, and caution must be exercised in extrapolating threshold values derived from younger rocks. Second, complications may arise from metamorphic and compositional effects that make it difficult to define the original depositional $Fe_{HR}$ contents of these rocks. Third, the Proterozoic oceans displayed considerable spatial and depth variability in composition, with weakly oxygenated surface waters overlying predominantly ferruginous water columns with mid-depth, near-shore euxinia (for example Poulton and others, 2004, 2010; and reviewed in Lyons and others, 2014). Multiple, basin-wide variations may require that all available proxy data are considered in a holistic context. This section begins by discussing how these challenges may be addressed for each of the different proxies.

We have seen that DOP values are robust and can be unaffected by burial/metamorphic alteration. Specifically, DOP values are calculated from Fe data derived from boiling HCl, which includes much iron present in minerals formed post-depositionally (whether syngenetic, diagenetic, or metamorphic) from phases that would have originally been reactive towards dissolved sulfide, carbonate, or silica in Precambrian sediments. Thus boiling HCl quantitatively removes all the iron present in the post-depositional silicates greenalite, stilpnomelane, and minesotaite but only 26 percent of the total iron in iron chlorite (chamosite). The failure to extract Fe as chamosite could potentially lead to an overestimate of DOP and threshold values need to be interpreted cautiously in this context.

The $Fe_T/Al$ ratio is clearly sensitive to iron enrichment (provided a baseline can be established). Ideally, the threshold is defined using oxic sediments in the particular geological/basinal setting. However, suitable oxic sediments may be difficult to identify in the Precambrian record, in part because oxic conditions were far less common. Enrichment may arise from the addition of Fe by a shelf-to-basin shuttle or by hydrothermal activity. Iron inputs in marginal marine basins and oceanic areas remote from hydrothermal activity can reasonably be interpreted as due to the operation of a shuttle. Nevertheless, it may still be difficult to recognize shuttle activity in oceanic settings where contemporaneous hydrothermal activity is occurring—because the influence of hydrothermal inputs into a ferruginous ocean can be widespread, in contrast to more localized impacts in a mostly oxic ocean.

As discussed earlier, critical issues with the $Fe_{HR}/Fe_T$ ratio relate to the methodology used to measure $Fe_{HR}$ and with the definitions of the oxic and anoxic thresholds. The thresholds were originally defined based on $Fe_{HR}$ as the sum of $Fe_{py}$ and $Fe_{ox}$, and oxic deposition was then proposed for settings with $Fe_{HR}/Fe_T < 0.38$, while anoxic (sulfidic and ferruginous) deposition was fingerprinted via $Fe_{HR}/Fe_T$ ratios $> 0.38$. This approach assumes that the contributions from iron carbonate and magnetite are minimal. However phases poorly soluble in dithionite (magnetite and some iron carbonates) are common in Precambrian sediments (and possibly also in Paleozoic sediments; see earlier). In these circumstances, a better measure of $Fe_{HR}$ is obtained as the sum of $Fe_{carb} + Fe_{ox} + Fe_{mag} + Fe_{py}$. In such cases, the original value of the oxic threshold at $< 0.38$ should be used with caution (bearing in mind that there have been no such measures of $Fe_{HR}$ for Precambrian sediments that have been independently verified as reflecting oxic deposition). A more conservative approach, based on observations of $Fe_{HR}/Fe_T$ in Paleozoic sediments, places the threshold for oxic deposition in ancient rocks at 0.22.

Euxinia is expressed in $Fe_{py}/Fe_{HR}$ ratios by near-complete consumption of $Fe_{HR}$ via pyrite formation. The original threshold, based on $Fe_{ox}$, defined euxinia by values

>0.80, but $Fe_{HR}$ measured as the sum of $Fe_{carb}$ + $Fe_{ox}$ + $Fe_{mag}$ + $Fe_{py}$ will be larger than $Fe_{ox}$ (significantly so if $Fe_{carb}$ and $Fe_{mag}$ are high). In these cases, a lower threshold (>0.70) is best used to recognize euxinia, with some uncertainty for values falling between 0.70 and 0.80 (Poulton and Canfield, 2011). We can explore these Precambrian complications below in a specific example.

### *The Mount McRae Shale*

The importance of considering multiple proxy indicators has been emphasized in recent studies of the McRae Shale, which consists of two pyritic, organic C-rich shales (the Lower and Upper Shale Units) interbedded with a sideritic banded iron formation and occasional carbonates (Kaufmann and others, 2007; Anbar and others, 2007). Iron speciation data (Reinhard and others, 2009) provided evidence for an anoxic water column that was mainly ferruginous but with euxinic intervals where oxidative weathering on the continents supplied sulfate for sulfate reduction, forming pyrite on the continental shelf. The following examples show how single proxy data are vulnerable to misinterpretation and how complementary data are needed to illuminate ambiguous signals in Precambrian rocks.

(i) Reinhard and others (2009) measured $Fe_{HR}$ content as the sum of $Fe_{carb}$ + $Fe_{ox}$ + $Fe_{mag}$ + $Fe_{py}$. Depth variations in $Fe_{HR}/Fe_T$ (fig. 12) show most samples lying close to the oxic/anoxic boundary at 0.38 except in the Upper Shale Interval (USI), where euxinia is indicated by DOP >0.75 and $Fe_{py}/Fe_{HR}$>0.70. The Lower Shale Interval (LSI) has values of $Fe_{HR}/Fe_T$ close to the 0.38 threshold, but $Fe_T/Al$ ratios are >1.0 in this unit which Reinhard and others (2009) considered to provide unequivocal evidence for iron addition and thus a ferruginous water column. The consideration of complementary $Fe_T/Al$ data by Reinhard and others (2009) avoided a potential pitfall.

The low $Fe_{HR}/Fe_T$ values in the LSI arose because carbonate Fe (ankerite and siderite) was only partially extracted by acetate and by oxalate. Thus, the estimates of $Fe_{HR}$ were too low, and $Fe_{HR}/Fe_T$ appeared close to the oxic threshold (fig. 12). The McRae carbonates can, however, be quantitatively extracted by cold 10 percent HCl (Raiswell and others, 2011), and the higher values of $Fe_{HR}$ then result in high $Fe_{HR}/Fe_T$ values that are unequivocally anoxic (fig. 12) and consistent with the $Fe_T/Al$ data. Methodologies should always be cross-checked to ensure that completion extraction has occurred.

(ii) The USI samples from approximately 140 to 150 m show consistently high values of DOP and $Fe_{py}/Fe_{HR}$ that Reinhard and others (2009) interpreted as euxinic based also on the abundance of Mo. High values of DOP and $Fe_{py}/Fe_{HR}$ on their own are not unambiguous evidence for euxinia because such results are also produced where ferruginous bottom waters occur over sulfidic porewaters. Molybdenum abundance in this case provided the crucial diagnostic evidence for euxinia, as it does in Case Study 4.

## SUMMARY AND RECOMMENDED APPROACH

A flowpath for decision making is illustrated in figure 13 and should be used in conjunction with the summary table for the proxy values (table 3).The text provides essential further details. Specifically, we encourage users of the Fe approach to:

1. Record the main geological features of the sequence to be studied—for example, depth of burial, basinal history, thermal maturity, and/or metamorphic grade. Collect thin sections of representative lithologies and determine mineralogy, grain size, *et cetera*.
2. Produce a stratigraphic section (see for example Sperling and others, 2016) that records grain size, color, bed characteristics, *et cetera*. The scale of the log should distinguish the sampled bed (or beds) and the presence of fossil

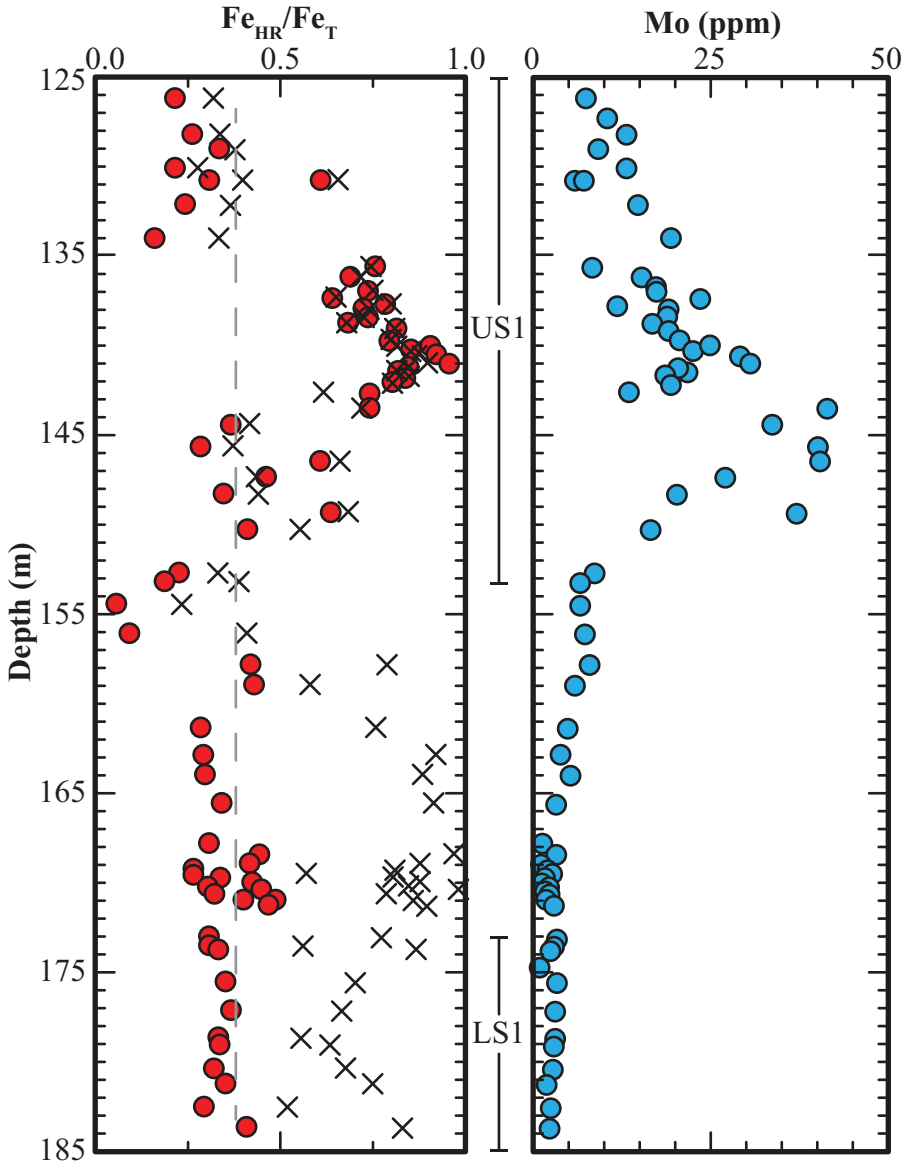


Fig. 12. Depth variations in $Fe_{HR}/Fe_T$ and Mo content in the Upper (USI) and Lower Shale intervals (LSI) of the McRae Shale. Red circles use $Fe_{HR}$ data from Reinhard and others (2009) and black crosses are $Fe_{HR}$ data from Raiswell and others (2011). The dashed line represents the anoxic threshold ($Fe_{HR}/Fe_T$ = 0.38).

material, veins, concretionary or coarse iron minerals, or any other conspicuous heterogeneities (see 3 below).

3. Aim to sample unweathered shales, siltstones, or carbonates (ideally core material) that are fine-grained and relatively dark in color, consistent with the presence of at least some organic matter and clays/silicates. Coarse sands and sandstones should be avoided. The analyses require ~0.5 g of sediment

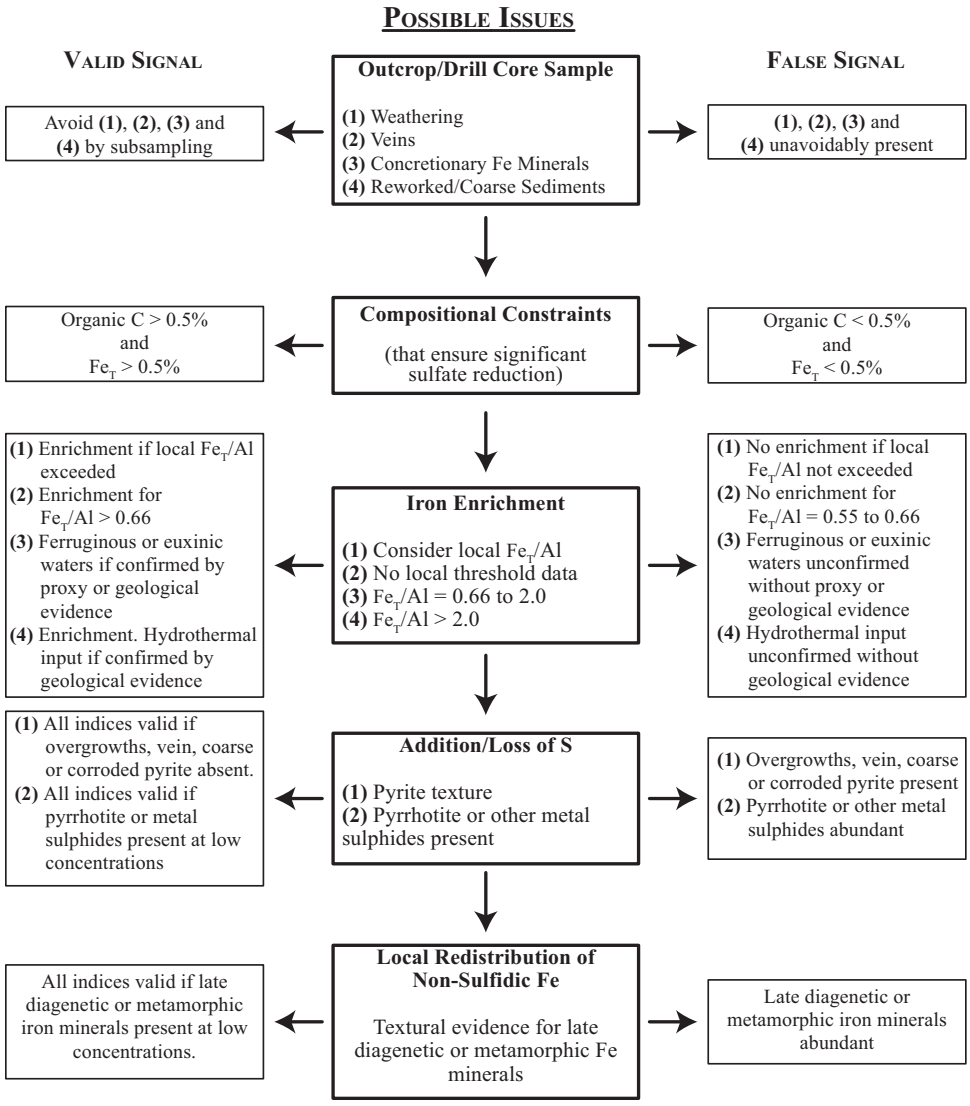


Fig. 13. Decision schematic for valid proxy interpretation.

(approximately equivalent to a cube with edges of ~5 mm). Grind away any weathered surfaces.

4. Study the samples for the presence of heterogeneities that may now be apparent on the freshly exposed faces. Crush the samples gently to produce grains very roughly around 1 mm in diameter and scan the fragments again for the presence of coarse iron minerals. Cut or handpick out any coarse minerals, such as macroscopic pyrite or veins. The aim is to collect representative samples rather than large, anomalous heterogeneities (nugget effects) that can skew the data. Crush samples to a powder.
5. Analyze samples for inorganic C and organic C, and total Fe and Al, pyrite sulfur, HCl-soluble Fe and dithionite-soluble Fe for $Fe_{ox}$ (as a minimum,

extractions specific to $Fe_{carb}$ and $Fe_{mag}$ may also be necessary; see text). Samples with $Fe_T > 0.5$ percent and organic C $< 0.5$ percent should be treated with caution.

6. Examine sediment texture and mineralogy for evidence of S addition or loss. Regional remobilization may be indicated by pyrite grain-size and texture and is most likely in thermally mature or metamorphosed sediments.
7. Examine sediment iron mineralogy for evidence of local Fe remobilization and the formation of late diagenetic and metamorphic Fe minerals (for example, magnetite, siderite, and iron silicates). Magnetite and siderite require the use of the Poulton and Canfield (2005) protocol. Local remobilization of Fe into iron silicates will invalidate all proxy data except DOP and $Fe_T/Al$, assuming that the secondary silicates are soluble in boiling HCl for DOP measurement.
8. Examine sediment sulfide mineralogy. The presence of iron monosulfides (AVS, pyrrhotite) require that $Fe_{HR}$ is calculated using the appropriate mineral stoichiometry. The presence of other sulfides related to secondary mineralization should be avoided (or removed by handpicking, if possible) during sampling and should be ignored during the derivation of $Fe_{HR}$ and $Fe_{py}$.
9. Examine proxy data. Table 3 provides a simple (not prescriptive) entry-point guide to proxy values, which should not be interpreted in isolation of the detailed discussions in the text. DOP values of $<0.45$ suggest an oxic or dysoxic environment and data $>0.75$ suggest a euxinic depositional environment. Oxic/dysoxic environments may be further confirmed by $Fe_{HR}/Fe_T < 0.22$ (ancient) or $<0.38$ (modern), although we caution that false positive signals for oxic/dysoxic conditions in the ancient record are possible, for example, under high rates of sedimentation. Values of $Fe_T/Al = 0.55 \pm 0.11$ can confirm oxic/dysoxic deposition provided the local source has similar values and there are no dilution effects from high sedimentation rate. Values of $Fe_T/Al > 0.66$ indicate anoxic deposition but require supporting proxy and/or geological evidence. Samples with $Fe_T/Al = 0.66–2.0$ should be examined for their $Fe_{HR}/Fe_T$ and $Fe_{py}/Fe_{HR}$ properties to demonstrate a ferruginous or euxinic depositional environment. Samples with $Fe_T/Al > 2.0$ require supporting geological evidence for/against local hydrothermal addition. Intermediate values of DOP require careful consideration of $Fe_T/Al$, $Fe_{HR}/Fe_T$, and $Fe_{py}/Fe_{HR}$, along with other proxy data, for an unambiguous interpretation—as they can reflect sulfidic pore fluids beneath oxic/dysoxic waters.

Despite the many caveats and considerations offered in this report, we end on an optimistic note. Many factors can control the distributions of reactive iron in marine sediments and sedimentary rocks, but we can minimize the risk of ambiguous interpretations when the diverse controlling factors are viewed within a multi-proxy context. Such an approach offers unique perspectives on, for example, rates of sedimentation and Fe source-sink relationships, and corresponding Fe capture pathways. At the same time, Fe-based constraints on local paleoredox allow us to interpret independent trace metal records in terms of seawater inventories modulated by local basinal restriction or the global redox landscape of the oceans and atmosphere. These and other opportunities explain why the Fe proxies have been and will continue to be at the center of studies aimed at the co-evolution of the oceans and their life.

## ACKNOWLEDGMENTS

The authors wish to thank the reviewers and especially Erik Sperling for his thorough and constructive comments. The authors also wish to acknowledge their funding support as follows; TL from the NSF FESD Program; TL, NP and CR from the NASA Astrobiology Institute under Cooperative Agreement No. NNA15BB03A issued

through the Science Mission Directorate; JO from NSF grant OCE 1434785 and the NASA Exobiology grant NNX16AJ60G; DC from Villum Foundation Grant No. 16518.

## APPENDIX

This appendix presents simple explanations for the terms commonly used in discussing the iron proxies. It is intended to make the text accessible to scientists without a formal background in sediment geochemistry and it should be used as only an entry point into the relevant literature.

*Acid Volatile Sulfide (AVS):* The operationally defined acid volatile sulfides consist of metastable iron sulfide minerals and dissolved sulfide species that emit $H_2S$ when treated with strong acids. AVS is largely transformed to pyrite during diagenesis.

*Anoxic:* Waters that contain no dissolved oxygen and may either contain dissolved iron (ferruginous) or dissolved sulfide (euxinic).

*Degree of Pyritization (DOP):* Defined as the ratio between pyrite Fe and the sum of pyrite Fe plus the iron soluble in concentrated boiling HCl. It was envisaged that all the iron minerals dissolved by HCl could react with dissolved sulfide (and thus a first attempt to estimate Highly Reactive Iron; see below). However this aggressive extraction dissolves a wide range of iron minerals some of which have little or no capacity to react to form pyrite.

*Degree of Sulfidation (DOS):* DOS is derived by the addition of Fe present as AVS (see above) to the numerator and denominator of DOP

$$\mathrm{DOS} = \frac{\text{Pyrite Fe} + \text{AVS Fe}}{\text{Pyrite Fe} + \text{AVS Fe} + \text{HCl–soluble Fe}}$$

DOS is often preferred over DOP for systems when AVS is present in appreciable amounts.

*Dysoxic:* Waters that contain low levels of dissolved oxygen (less than saturation levels) but are neither ferruginous nor sulfidic.

*Euxinic:* Anoxic waters that contain dissolved sulfide and negligible concentrations of dissolved iron.

*Ferruginous:* Anoxic waters that contain dissolved iron and negligible concentrations of dissolved sulfide.

*Highly Reactive Iron:* The iron present as sediment minerals that are capable of reacting with dissolved sulfide to form pyrite or AVS. Estimated as the sum of pyrite iron (which has formed from iron minerals that have already reacted with dissolved sulfide) plus the iron present as the (oxyhydr)oxide minerals soluble in dithionite. It is now accepted, however, that highly reactive iron also includes the minerals siderite, magnetite and ankerite, in addition to iron (oxyhydr)oxides.

*Indicator of Anoxicity:* Defined as the ratio between (Highly Reactive Iron)/Total Fe, where highly reactive iron is measured as pyrite Fe plus the Fe soluble in dithionite. This term is now largely obsolete as Highly Reactive Iron is more correctly defined to include siderite, magnetite and ankerite (see Highly Reactive Iron).

*Iron Shuttle:* Iron enrichments in the deep basinal euxinic sediments are sourced by microbial Fe reduction in oxic shelf sediments, diffusion of reduced iron into the overlying waters, followed by transport of a proportion of the resulting iron (now oxidized to Fe (oxyhydr)oxides or still dissolved) to the deep basin, where it is captured by the sulfidic water column and precipitated as pyrite.

*Pyrite Iron:* The iron present as pyrite, excluding AVS. The $H_2S$ produced by sulfate reduction reacts with Fe minerals to form FeS (measured as AVS), which then reacts with partially oxidized sulfide species or $H_2S$. FeS can also react directly with $H_2S$ to produce pyrite.

## REFERENCES

Ahm, A-S., Bjerrum, C. J., and Hammarlund, E. U., 2017, Disentangling the record of diagenesis, local redox conditions, and global seawater chemistry during the latest Ordovician glaciation: Earth and Planetary Science Letters, v. 459, p. 145–156, https://doi.org/10.1016/j.epsl.2016.09.049

Aller, R. C., Mackin, J. E., and Cox, R. T., Jr., 1986, Diagenesis of Fe and S in Amazon inner shelf muds: Apparent dominance of iron reduction and implications for the genesis of ironstones: Continental Shelf Research, v. 6, n. 1–2, p. 263–289, https://doi.org/10.1016/0278-4343(86)90064-6

Anbar, A. D., Duan, Y., Lyons, T. W., Arnold, G. L., Kendall, B., Creaser, R. A., Kaufman, A. J., Gordon, G. W., Scott, C., Garvin, J., and Buick, R., 2007, A whiff of oxygen before the Great Oxidation Event?: Science, v. 377, n. 5846, p. 1903–1906 https://doi.org/10.1126/science.1140325

Anderson, R. F., Lyons, T. W., and Cowie, G. L., 1994, Sedimentary record of a shoaling of the oxic/anoxic interface in the Black Sea: Marine Geology, v. 116, n. 3–4, p. 373–384, https://doi.org/10.1016/0025-3227(94)90052-3

Anderson, T. F., and Raiswell, R., 2004, Sources and mechanisms for the enrichment of highly reactive iron in euxinic Black Sea sediments: American Journal of Science, v. 304, n. 3, p. 203–233, https://doi.org/10.2475/ajs.304.3.203

Andrén, T., Björck, S., Andrén, E., Conley D., Zillen, L., and Anjar, J., 2011, The development of the Baltic

Sea Basin during the last 130 ka, *in* Harff. J., Björck, J., and Hoth, P., editors, The Baltic Sea Basin: Berlin, Springer, Central and Eastern European Development Studies, p. 75–97, http://dx.doi.org/10.1007/978-3-642-17220-5_4

Asael, D., Tissot, F. L. H., Reinhard, C. T., Rouxel, O., Dauphas, N., Lyons, T. W., Ponzevera, E., Liorzou, C., and Cheron, S., 2013, Coupled molybdenum, iron and uranium stable isotopes as oceanic paleoredox proxies during the Paleoproterozoic Shunga Event: Chemical Geology, v. 362, p. 193–210, https://doi.org/10.1016/j.chemgeo.2013.08.003

Berner, R. A., 1969, Migration of iron and sulfur within anaerobic sediments during early diagenesis: American Journal of Science, v. 267, n. 1, p. 19–42, https://doi.org/10.2475/ajs.267.1.19

——— 1970, Sedimentary pyrite formation: American Journal of Science, v. 268, n. 1, p. 1–23, https://doi.org/10.2475/ajs.268.1.1

——— 1984, Sedimentary pyrite formation: An update: Geochimica et Cosmochimica Acta, v. 48, n. 4, p. 605–615, https://doi.org/10.1016/0016-7037(84)90089-9

Boesen, C., and Postma, D., 1988, Pyrite formation in anoxic environments of the Baltic: American Journal of Science, v. 288, n. 6, p. 575–603, https://doi.org/10.2475/ajs.288.6.575

Boyer, D. L., Owens, J. D., Lyons, T. W., and Droser, M. L., 2011, Joining forces: Combined biological and geochemical proxies reveal a complex but refined high-resolution palaeo-oxygen history in Devonian epeiric seas: Palaeogeography, Palaeoclimatology, and Palaeoecology, v. 306, n. 3–4, p. 134–146, https://doi.org/10.1016/j.palaeo.2011.04.012

Canfield, D. E., 1989, Reactive iron in marine sediments: Geochimica et Cosmochimia Acta, v. 53, n. 3, p. 619–632, https://doi.org/10.1016/0016-7037(89)90005-7

Canfield, D. E., Raiswell, R., Westrich, J. T., Reaves, C. M., and Berner, R. A., 1986, The use of chromium reduction in the analysis of reduced inorganic sulfur in sediments and shales: Chemical Geology, v. 54, n. 1–2, p. 149–155, https://doi.org/10.1016/0009-2541(86)90078-1

Canfield, D. E., Raiswell, R., and Bottrell, S., 1992, The reactivity of sedimentary iron minerals toward sulfide: American Journal of Science, v. 292, n. 9, p. 659–683, https://doi.org/10.2475/ajs.292.9.659

Canfield, D. E., Lyons, T. W., and Raiswell, R., 1996, A model for iron deposition to euxinic Black Sea sediments: American Journal of Science, v. 296, n. 7, p. 818–834, https://doi.org/10.2475/ajs.296.7.818

Canfield, D. E., Poulton, S. W., Knoll, A. H., Narbonne, G. M., Ross, G., Goldberg, T., and Strauss, H., 2008, Ferruginous conditions dominated later Neoproterozoic deep water chemistry: Science, v. 321, n. 5891, p. 949–952, https://doi.org/10.1126/science.1154499

Chever, F., Rouxel, O. J., Croot, P. L., Ponzevera, E., Wuttig, K., and Auro, M., 2015, Total dissolvable and dissolved iron isotopes in the water column of the Peru upwelling regime: Geochimica et Cosmochimica Acta, v. 162, p. 66–82, https://doi.org/10.1016/j.gca.2015.04.031

Clarke, F. W., 1924, Data on Geochemistry: United States Geological Survey, n. 770, 839 p.

Clarkson, M. O., Poulton, S. W., Guilbaud, R., and Wood, R., 2014, Assessing the utility of Fe/Al and Fe-speciation to record water column redox conditions in carbonate-rich sediments: Chemical Geology, v. 382, p. 111–122.

Cole, D. B., Zhang, S., and Planavsky, N. J., 2017, A new estimate of detrital redox-sensitive metal concentrations and variability in fluxes to marine sediments: Geochimica et Cosmochimica Acta, v. 215, p. 337–353, https://doi.org/10.1016/j.gca.2017.08.004

Cruse, A. M., and Lyons, T. W, 2004, Trace metal records of regional paleoenvironmental variability in Pennsylvanian (Upper Carboniferous) black shales: Chemical Geology, v. 206, n. 34, n. 3–4, p. 319–345, https://doi.org/10.1016/j.chemgeo.2003.12.010

Crusius, J., and Anderson, R. F., 1991, Immobility of $^{210}$Pb in Black Sea sediments: Geochimica et Cosmochimica Acta, v. 55, n. 1, p. 327–333, https://doi.org/10.1016/0016-7037(91)90421-Z

Cumming, V. M., Poulton, S. W., Rooney, A. D., and Selby, D., 2013, Anoxia in the terrestrial environment during the late Mesoproterozoic: Geology, v. 41, n. 5, p. 583–586, https://doi.org/10.1130/G34299.1

Farrell, U. C., Briggs, D. E. G., Hammerlund, E. U., Sperling, E. A., and Gaines, R. R., 2013, Paleoredox and pyritization of soft-bodied fossils in the Ordovician Frankfurt Shale of New York: American Journal of Science, v. 313, n. 5, p. 452–489, https://doi.org/10.2475/05.2013.02

Fehr, M. A., Andersson, P. S., Halenius, U., and Mörth, C-M., 2008, Iron isotope variations in Holocene sediments of the Gotland Deep, Baltic Sea: Geochimica et Cosmochimica Acta, v. 72, n. 3, p. 807–826, https://doi.org/10.1016/j.gca.2007.11.033

Goldberg, T., Archer, C., Vance, D., Thamdrup, B., McAnena, A., and Poulton, S. W., 2012, Controls on Mo isotope fractionations in a Mn-rich anoxic marine sediment, Gullmar Fjord, Sweden: Chemical Geology, v. 296, p. 73–82, https://doi.org/10.1016/j.chemgeo.2011.12.020

Goldhaber, M. B., Aller, R. C., Cochran, J. K., Rosenfeld, J. K., Martens, C. S., and Berner, R. A., 1977, Sulfate reduction, diffusion and bioturbation in Long Island Sound sediments: Report of the FOAM group: American Journal of Science, v. 277, n. 3, p. 193–237, https://doi.org/10.2475/ajs.277.3.193

Hardisty, D. S., Riedinger, N., Planavsky, N. J., Asael, D., Andren, T., Jorgensen, B. B., and Lyons, T. W., 2016, A Holocene history of dynamic water column redox conditions in the Landsort Deep, Baltic Sea: American Journal of Science, v. 316, n. 8, p. 713–745, https://doi.org/10.2475/08.2016.01

Hardisty, D. S., Lyons, T. W., Riedinger, N., Isson, T. T., Owens, J. O., Aller, R. C., Rye, D. M., Planavsky, N. J., Reinhard, C. T., Gill, B. C., Masterson, A. L., Asael, D., and Johnston, D. T., 2018, An evaluation of sedimentary molybdenum and iron as proxies for pore fluid paleoredox conditions: American Journal of Science, v. 318, n. 5, https://doi.org/10.2475/05.2018.04

Holmkvist, L., Kamyshny, A., Jr., Brüchert, V., Ferdelman, T. G., and Jørgensen, B. B., 2014, Sulfidization of lacustrine glacial clay upon Holocene marine transgression (Arkona Basin, Baltic Sea): Geochimica et Cosmochimica Acta, v. 142, p. 75–94, https://doi.org/10.1016/j.gca.2014.07.030

Hurtgen, M. T., Lyons, T. W., Ingall, E. D., and Cruse, A. M., 1999, Anomalous enrichments of iron

monosulfide in euxinic marine sediments and the role of $H_2S$ in iron sulfide transformations: Examples from Effingham Inlet, Orca Basin, and the Black Sea: American Journal of Science, v. 299, n. 7–9, p. 556–588, https://doi.org/10.2475/ajs.299.7-9.556

Jia, Y., 2006, Nitrogen isotope fractionations during progressive metamorphism: A case study from the Paleozoic Cooma metasedimentary complex, southeastern Australia: Geochimica et Cosmochimica Acta, v. 70, n. 20, p. 5201–5214, https://doi.org/10.1016/j.gca.2006.08.004

Jilbert, T., and Slomp, C. P , 2013, Rapid high-amplitude variability in Baltic Sea hypoxia during the Holocene: Geology, v. 41, n. 11, p. 1183–1186, https://doi.org/10.1130/G34804.1

Jones, C. E., and Jenkyns, H. C., 2001, Seawater strontium isotopes, oceanic anoxic events, and seafloor hydrothermal activity in the Jurassic and Cretaceous: American Journal of Science, v. 301, n. 2, p. 112–149, https://doi.org/10.2475/ajs.301.2.112

Jorgensen, B. B., Bottcher, M. E., Luschen, H., Neretin, N. L., and Volkov, I. I., 2004, Anaerobic methane oxidation and a deep $H_2S$ sink generate isotopically heavy sulfides in black Sea sediments: Geochimica et Cosmochimica Acta, v. 68, n. 9, p. 2095–2118, https://doi.org/10.1016/j.gca.2003.07.017

Kaufman, A. J., Johnston, D. T., Farquhar, J., Masterson, A. L., Lyons, T. W., Bates, S., Anbar, A. D., Arnold, G. L., Garvin, J., and Buick, R., 2007, Late Archean biospheric oxygenation and atmospheric evolution: Science, v. 317, n. 5846, p. 1900–1903, https://doi.org/10.1126/science.1138700

Krishnaswami, S., Monaghan, M. C., Westrich, J. T., Bennett, J. T., and Turekian, K. K., 1984, Chronologies of sedimentary processes in sediments of the FOAM site, Long Island Sound, Connecticut: American Journal of Science, v. 284, n. 6, p. 706–733, https://doi.org/10.2475/ajs.284.6.706

Lepland, A., and Stevens, R. L., 1998, Manganese authigenesis in the Landsort Deep, Baltic Sea: Marine Geology, v. 151, n. 1–4, p. 1–25, https://doi.org/10.1016/S0025-3227(98)00046-2

Lyons, T. W., 1997, Sulfur isotope trends and pathways of iron sulfide formation in the Upper Holocene sediments of the anoxic Black Sea: Geochimica et Cosmochimica Acta, v. 61, n. 16, p. 3367–3382, https://doi.org/10.1016/S0016-7037(97)00174-9

Lyons, T. W., and Berner, R. A., 1992, Carbon-sulfur-iron systematics of the uppermost deep-water sediments of the Black Sea: Chemical Geology, v. 99, n. 1–3, p. 1–27, https://doi.org/10.1016/0009-2541(92)90028-4

Lyons, T. W., and Severmann, S., 2006, A critical look at iron paleoredox proxies: New insights from modern euxinic marine basins: Geochimica et Cosmochimica Acta, v. 70, n. 23, p. 5698–5722, https://doi.org/10.1016/j.gca.2006.08.021

Lyons, T. W., Werne, J. P., Hollander, D. J., and Murray, J. W., 2003, Contrasting sulfur geochemistry and Fe/Al and Mo/Al ratios across the last oxic-to-anoxic transition in the Cariaco Basin, Venezuela: Chemical Geology, v. 195, n. 1–4, p. 131–157, https://doi.org/10.1016/S0009-2541(02)00392-3

Lyons, T. W., Anbar, A. D., Severmann, S., Scott, C., and Gill, B. C., 2009,Tracking euxinia in the ancient ocean: A multiproxy perspective and Proterozoic case study: Annual Reviews of Earth and Planetary Sciences, v. 37, p. 507–534, https://doi.org/10.1146/annurev.earth.36.031207.124233

Lyons, T. W., Reinhard, C. T., and Planavsky, N. J., 2014, The rise of oxygen in the Earth's early ocean and atmosphere: Nature, v. 506, p. 307–315, https://doi.org/10.1038/nature13068

März, C., Poulton, S. W., Beckmann, B., Küster, K., Wagner, T., and Kasten, S., 2008, Redox sensitivity of P cycling during marine black shale formation: Dynamics of sulfidic and anoxic, non-sulfidic bottom waters: Geochimica et Cosmochimica Acta, v. 72, n. 15, p. 3703–3717, https://doi.org/10.1016/j.gca.2008.04.025

März, C., Poulton, S. W., Brumsack, H-J., and Wagner, T., 2012, Climate-controlled variability of iron deposition in the Central Arctic Ocean (southern Mendeleev Ridge) over the last 130,000 years: Chemical Geology, v. 330–331, p. 116–126, https://doi.org/10.1016/j.chemgeo.2012.08.015

Middelburg, J. J., 1991, Organic carbon, sulphur, and iron in recent semi-euxinic sediments of Kau Bay, Indonesia: Geochimica et Cosmochimica Acta, v. 55, n. 3, p. 815–828, https://doi.org/10.1016/0016-7037(91)90344-5

Owens, J. D., Lyons, T. W., Li, X., Macleod, K. G., Gordon, G., Kuypers, M. M. M., Anbar, A., Kuht, W., and Severmann, S., 2012, Iron isotope and trace metal records of iron cycling in the proto-North Atlantic during the Cenomanian-Turonian oceanic anoxic event (OAE-2): Paleoceanography, v. 27, PA3223, doi:10.1029/2012/PA002328.

Passier, H. F., Middelburg, J. J., van Os, B. J. H., and de Lange, G. J., 1996, Diagenetic pyritisation under eastern Mediterranean sapropels caused by downward sulfide diffusion: Geochimica et Cosmochimica Acta, v. 60, n. 5, p. 751–763, https://doi.org/10.1016/0016-7037(95)00419-X

Planavsky, N. J., McColdrick, P., Scott, C. T., Li, C., Reinhard, C. T., Kelly, A. E., Chu, X., Bekker, A., Love, G. D., and Lyons, T. W., 2011, Widespread iron-rich conditions in the mid-Proterozoic ocean: Nature, v. 477, p. 478–451, https://doi.org/10.1038/nature10327

Poulton, S. W., and Canfield, D. E., 2005, Development of a sequential extraction procedure for iron: Implications for iron partitioning in continentally derived particulates: Chemical Geology, v. 214, n. 3–4, p. 209–211, https://doi.org/10.1016/j.chemgeo.2004.09.003

——— 2011, Ferruginous conditions: A dominant feature of the ocean through Earth's history: Elements, v. 7, n. 2, p. 107–112, https://doi.org/10.2113/gselements.7.2.107

Poulton, S. W., and Raiswell, R., 2002, The low temperature geochemical cycle of iron: From continental fluxes to marine sediment deposition: American Journal of Science, v. 302, n. 9, p. 774–805, https://doi.org/10.2475/ajs.302.9.774

Poulton, S. W., Fralick, P. W., and Canfield, D. E., 2004, The transition to a sulfidic ocean ~1.84 billion years ago: Nature, v. 431, p. 173–177, https://doi.org/10.1038/nature02912

——— 2010, Spatial variability in oceanic redox structure 1.8 billion years ago: Nature Geoscience, v. 3, p. 486–490, https://doi.org/10.1038/ngeo889

Raiswell, R., and Al-Biatty, H. J., 1989, Depositional and diagenetic C-S-Fe signatures in early Paleozoic

normal marine shales: Geochimica et Cosmochimica Acta, v. 53, n. 5, p. 1147–1152, https://doi.org/10.1016/0016-7037(89)90220-2
Raiswell, R., and Anderson, T. F., 2005, Reactive iron enrichment in sediments deposited beneath euxinic bottom waters: Constraints on supply by shelf re-cycling, *in* McDonald, I., Boyce, A. J., Butler, I. B., Herrington, R. J., and Polya, D. A., editors, Mineral Deposits and Earth Evolution: Geological Society, London, Special Publications, v. 218, p. 179–194, https://doi.org/10.1144/GSL.SP.2005.248.01.10
Raiswell, R., and Berner, R. A., 1985, Pyrite formation in euxinic and semi-euxinic sediments: American Journal of Science, v. 285, n. 8, p. 710–724, https://doi.org/10.2475/ajs.285.8.710
——— 1986, Pyrite and organic matter in Phanerozoic normal marine shales: Geochimica et Cosmochimica Acta, v. 50, n. 9, p. 1967–1976, https://doi.org/10.1016/0016-7037(86)90252-8
Raiswell, R., and Canfield, D. E., 1996, Rates of reaction between silicate iron and dissolved sulfide in Peru Margin sediments: Geochimica et Cosmochimica Acta, v. 60, n. 15, p. 2777–2787, https://doi.org/10.1016/0016-7037(96)00141-X
——— 1998, Sources of iron for pyrite formation in marine sediments: American Journal of Science, v. 298, n. 3, p. 219–243, https://doi.org/10.2475/ajs.298.3.219
——— 2012, The iron biogeochemical cycle past and present, Geochemical Perspectives, v. 1, n. 1, p. 1–220, https://doi.org/10.7185/geochempersp.1.1
Raiswell, R., Buckley, F., Berner, R. A., and Anderson, T. F., 1988, Degree of pyritization of iron as a paleoenvironmental indicator: Journal of Sedimentary Petrology, v. 58, n. 5, p. 812–819, https://doi.org/10.1306/212F8E72-2B24-11D7-8648000102C1865D
Raiswell, R., Canfield, D. E., and Berner, R. A., 1994, A comparison of iron extraction methods for the determination of degree of pyritisation and the recognition of iron-limited pyrite formation: Chemical Geology, v. 111, n. 1–4, p. 101–111, https://doi.org/10.1016/0009-2541(94)90084-1
Raiswell, R., Newton, R., and Wignall, P. B., 2001, An indicator of water column anoxia: Resolution of biofacies variations in the Kimmeridge clay (Upper Jurassic, UK): Journal of Sedimentary Research, v. 71, n. 2, p. 286–294, https://doi.org/10.1306/070300710286
Raiswell, R., Newton, R., Bottrell, S. H., Coburn, P. M., Briggs, D. E. G., Bond, D. P. G., and Poulton, S. W., 2008, Turbidite depositional influences on the diagenesis of Beecher's Trilobite Bed and the Hunsrück Slate: Sites of soft tissue preservation: American Journal of Science, v. 308, n. 2, p. 105–129, https://doi.org/10.2475/02.2008.01
Raiswell, R., Reinhard, C. T., Derkowski, A., Owens, J., Bottrell, S. H., Anbar, A. D., and Lyons, T. W., 2011, Formation of syngenetic and early diagenetic iron minerals in the late Archean Mt. McRae Shale, Hamersley Basin, Australia: New insights on the patterns, controls and paleoenvironmental implications of authigenic mineral formation: Geochimica et Cosmochimica Acta, v. 75, n. 4, p. 1072–1087, https://doi.org/10.1016/j.gca.2010.11.013
Raiswell, R., Hawkings, J. R., Benning, L. G., Baker, A. R., Death, R., Albani, S., Mahowald, N., Krom, M. D., Poulton, S. W., Wadham, J., and Tranter, M., 2016, Potentially bioavailable iron delivery by iceberg-hosted sediments and atmospheric dust to the polar oceans: Biogeosciences, v. 13, n. 13, p. 3887–3900, https://doi.org/10.5194/bg-13-3887-2016
Reinhard, C. T., Raiswell, R., Scott, C., Anbar, A. D., and Lyons, T. W., 2009, A late Archean sulfidic sea stimulated by early oxidative weathering of the continents: Science, v. 326, n. 5953, p. 713–716, https://doi.org/10.1126/science.1176711
Reinhard, C. T., Lyons, T. W., Rouxel, O., Asael, D., Dauphas, N., and Kump, L. R., 2013, Iron speciation and isotope perspectives on Paleoproterozoic water column chemistry, *in* Melezhik, V., Prave, A. R., Hanski, E. J., Fallick, A. E., Lepland, A., Kump, L. R., and Strauss, H., editors, Reading the Archive of Earth's Oxygenation: Berlin, Springer, p. 1483–1492.
Ronov, A. B., and Migdisov, A. A., 1971, Geochemical history of the crystalline basement and the sedimentary cover of the Russian and North American platforms: Sedimentology, v. 16, n. 3–4, p. 1775–1785, https://doi.org/10.1111/j.1365-3091.1971.tb00227.x
Rozonov, A. G., Volkov, I. I., and Yagodinskaya, T. A., 1974, Forms of iron in the surface layer of Black Sea sediments, *in* Degens, E. T., and Ross, D. A., editors, The Black Sea–Geology, Chemistry, and Biology: Tulsa, Oklahoma, American Association of Petroleum Geology Memoir, v. 20, p. 532–541, https://doi.org/10.1306/M20377C16
Scholz, F., Severmann, S., McManus, J., and Hensen, C., 2014a, Beyond the Black Sea paradigm: The sedimentary fingerprint of an open-marine iron shuttle: Geochimica et Cosmochimica Acta, v. 127, p. 368–380, https://doi.org/10.1016/j.gca.2013.11.041
Scholz, F., Severmann, S., McManus, J., Noffke, A., Lomnitz, U., and Hensen, C., 2014b, On the isotope composition of reactive iron in marine sediments: Redox shuttle versus early diagenesis: Chemical Geology, v. 389, p. 48–59, https://doi.org/10.1016/j.chemgeo.2014.09.009
Scott, C., and Lyons, T. W., 2012, Contrasting molybdenum cycling and isotopic properties in euxinic versus non-euxinic sediments and sedimentary proxies: Refining the paleoproxies: Chemical Geology, v. 324–325, p. 19–27, https://doi.org/10.1016/j.chemgeo.2012.05.012
Scott, C., Lyons, T. W., Bekker, A., Shen, Y., Poulton, S. W., Chu, X., and Anbar, A. D., 2008, Tracing the stepwise oxygenation of the Proterozoic ocean: Nature, v. 452, p. 456–459, https://doi.org/10.1038/nature06811
Severmann, S., Lyons, T. W., Anbar, A., McManus, J., and Gordon, G., 2008, Modern iron isotope perspective on the benthic iron shuttle and the redox evolution of ancient oceans: Geology, v. 36, n. 6, p. 487–490, https://doi.org/10.1130/G24670A.1
Severmann, S., McManus, J., Berelson, W. M., and Hammond, D. E., 2010, The continental shelf benthic iron flux and its isotopic composition: Geochimica et Cosmochimica Acta, v. 74, n. 14, p. 3984–4004, https://doi.org/10.1016/j.gca.2010.04.022
Shi, Z., Krom, M. D., Bonneville, S., Baker, A. R., Bristow, C., Drake, N., Mann, G., Carslaw, K., McQuaid,

J. B., Jickells, T., and Benning, L. G., 2011, Influence of chemical weathering and aging of iron oxides on the potential iron solubility of Saharan dust during simulated atmospheric processing: Global Biogeochemical Cycles, v. 25, n. 2, GB2010, https://doi.org/10.1029/2010GB003837

Slotznick, S. P., Winston, D., Webb, S. M., Kirscchvink, J. L., and Fischer, W. W., 2016, Iron mineralogy and redox conditions during deposition of the mid-Proterozoic Appekunny Formation, Belt Supergroup, Glacier National Park: Geological Society of America Special Paper, n. 522, v. 221–242, https://doi.org/10.1130/2016.2522(09)

Slotznick, S. P., Eiler, J. M., and Fischer, W. W., 2018, The effects of metamorphism on iron mineralogy and the iron speciation redox proxy: Geochimica et Cosmochimca Acta, v. 224, p. 96–115, https://doi.org/10.1016/j.gca.2017.12.03

Sohlenius, G., Sternback, J., Andrén, E., and Westman, P., 1996, Holocene history of the Baltic Sea as recorded in a sediment core from the Gotland deep: Marine Geology, v. 134, n. 3–4, p. 183–201, https://doi.org/10.1016/0025-3227(96)00047-3

Sohlenius, G., Emeis, K-C., Andrén, E., Andrén, T., and Kohly, A., 2001, Development of anoxia during the Holocene fresh–brackish water transition in the Baltic Sea: Marine Geology, v. 177, n. 3–4, p. 221–242, https://doi.org/10.1016/S0025-3227(01)00174-8

Sperling, E. A., Halverson, G. P., Knoll, A. H., Macdonald, F. A., and Johnston, D. T., 2013, A basin redox transect at the dawn of animal life: Earth and Planetary Science Letters, v. 371–372, p. 143–155, https://doi.org/10.1016/j.epsl.2013.04.003

Sperling, E. A., Wolock, C. J., Morgan, A. S., Gill, B. C., Kunzmann, M., Halverson, G. P., Macdonald, F. A., Knoll, A. H., and Johnston, D. T., 2015, Statistical analysis of iron geochemical data suggests limited late Proterozoic oxygenation: Nature, v. 523, p. 451–454, https://doi.org/10.1038/nature14589

Sperling, E. A., Carbonne, C., Strauss, J. V., Johnston, D. T., Narbonne, G. M,, and Macdonald, F. A., 2016, Oxygen, facies, and secular controls on the appearance of Cryogenian and Ediacaran body and trace fossls in the Mackenzie Mountains of northwestern Canada: Geological Society of America Bulletin, v. 128, n. 3–4, p. 558–575, https://doi.org/10.1130/B31329.1

Taylor, S. R., and McLennan, S. M., 1985, The Continental Crust: Its Composition and Evolution: Oxford, Blackwell, 312 p.

Trefry, J. H., Presley, B. J., Keeney-Kennicutt, W. L., and Trocine, R. P., 1984, Distribution and chemistry of manganese, iron, and suspended particulates in Orca Basin: Geo-Marine Letters, v. 4, n. 2, p. 125–130, https://doi.org/10.1007/BF02277083

Van Cappellen, P., Violler, E., Roychoudbury, A., Clark, L., Ingall, E., Lowe K., and Dichristina, T., 1998, Biogeochemical cycles of manganese and iron at the oxic-anoxic transition of a stratified marine basin (Orca Basin, Gulf of Mexico): Environmental Science and Technology, v. 32, n. 19, p. 2931–2939, https://doi.org/10.1021/es980307m

Wen, H., Carignan, J., Chu, X., Fan, H., Cloquet, C., Huang, J., Zhang, Y., and Chang, H., 2014, Selenium isotopes trace anoxic and ferruginous seawater conditions in the Early Cambrian: Chemical Geology, v. 390, p. 164–172, https://doi.org/10.1016/j.chemgeo.2014.10.022

Werne, J. P., Sageman, B. B., Lyons, T. W., and Hollander, D. J., 2002, An integrated assessment of a type 'euxinic' deposit: Evidence for multiple controls on black shale deposition in the Middle Devonian Oatka Creek Formation: American Journal of Science, v. 302, n. 2, p. 110–143, https://doi.org/10.2475/ajs.302.2.110

Wijsman, J. W. M., Middleberg, J. J., and Heip, C. H. R., 2001, Reactive iron in Black Sea sediments: Implications for iron cycling: Marine Geology, v. 172, n. 3–4, p. 167–180, https://doi.org/10.1016/S0025-3227(00)00122-5

Yui, T-F., Kao, S-J., and Wu, T-W., 2009, Nitrogen and N-isotope variation during low-grade metamorphism of the Taiwan mountain belt: Geochemical Journal, v. 43, n. 1, p. 15–27, https://doi.org/10.2343/geochemj.1.0003

Zillén, L., Conley, D. J., Andrén, T., Andrén, E., and Björck, S., 2008, Past occurrences of hypoxia in the Baltic Sea and the role of climate variability, environmental change and human impact: Earth Science Reviews, v. 91, n. 1–4, p. 77–92, https://doi.org/10.1016/j.earscirev.2008.10.001